平 成 **22** 年 度

博士学位論文

# EDLC FROM ACTIVATED CARBON DERIVED FROM BLACK LIQUOR

**Xiao-Yan Zhao**

DOCTORAL DISSERTATION

# EDLC FROM ACTIVATED CARBON DERIVED FROM BLACK LIQUOR

(黒液からの活性炭製造と電気二重層キャパシタの応用)

By
Xiao-Yan Zhao

Gunma University, Faculty of Engineering
Department of Chemical and Environmental Engineering
*Gunma, Kiryu, Tenjin-cho 1-5-1, 376-8515, Japan*

# Evaluation Committee

Professor Takayuki TAKARADA, Chair

Professor Shinji KATSURA

Professor Jun-ichi OZAKI

Associate Professor Masaru HAKODA

Associate Professor Reiji NODA

*Faculty of Engineering, Gunma University, JAPAN*

# Abstract

Using black liquor as a porous carbon precursor is considered as an effective approach for value-added use of black liquor. In addition, black liquor contains high content of alkali metals (Na, K, etc.), which are effectively used to improve the activation process. Therefore, preparation of activated carbons (ACs) directly from black liquor may reduce the cost not only for lignin-recycling, but also for activating agents economizing. Electric double-layer capacitors (EDLCs) are very attractive as a potential energy storage system because of their high power density, quick charge-discharge rate, free maintenance, long-life operation, and environmentally friendly energy technology. EDLCs with activated carbon electrodes are known to have higher capacity for energy storage compared with conventional condensers. However, the application of ACs derived from black liquor for the preparation of EDLCs has not been reported previously.

In chapter 2, high surface area ACs were prepared by chemical activation of black liquor with potassium hydroxide (KOH), sodium hydroxide (NaOH) and potassium carbonate ($K_2CO_3$). The influence of carbonization temperature, activation temperature, holding time and impregnation ratio of activating agent to char on the porous characteristics of the ACs was investigated. The results show that the surface area and pore volume of ACs, which were estimated by BET methods, were achieved as high as 3089 $m^2$ $g^{-1}$ and 1.76 $cm^3$ $g^{-1}$ four times larger than a commercial AC from charcoal (944 $m^2$ $g^{-1}$), under the condition of an carbonization temperature of 600 $^oC$, an activation temperature of 900 $^oC$, a holding time of 2 h and an impregnation ratio (KOH/Char) of 2. In addition, the

influence of alkali metals (K and Na) existing in black liquor on activation was also examined. It was found that the alkali metals react as an activating agent in the process of activation, thereby economizing the amount of activating agent used in this study to a high degree.

In chapter 3, the performance of ACs derived from black liquor as EDLCs was characterized. The gravimetric capacitance is found to be approximately proportional to the BET surface area, and the AC with the maximum gravimetric capacitance of 41.4 F $g^{-1}$ and the maximum volumetric capacitance of 16.6 F $cm^{-3}$ was developed under the preparing condition of an carbonization of 600 $^{o}$C, an activation temperature of 600 $^{o}$C, a holding time of 2 h and an impregnation ratio (KOH/Char) of 2. In addition, the results obtained in this study confirm that capacitance of ACs from black liquor not only depends on surface area, but also on pore size. This study provides an effective approach to carry out the value-added utilization of black liquor.

# TABLE OF CONTENTS

# Chapter 1 Introduction

## 1.1 Black Liquor


**Figure 1–1 Black liquor**

Black liquor, a mixture of organic wastes, is a by-product of the paper making process.[1–4] Black liquor is an important liquid fuel in the pulp and paper industry, consists of the remaining substances after the digestive process where the cellulose fibers have been cooked out from the wood.[5] And it's routinely burned as a liquid fuel in a recovery boiler in a pulp mill. Approximately 1.5 tones of black liquor are produced in the manufacture of 1 tone of pulp. Generally, a calorimetric heat value of Kraft black liquor is 12.6 MJ/kg and its energy is mainly used for pulp and paper making process.[6] The shape of black liquor is given in **Figure 1–1**.

### 1.1.1 Paper Making Process

Nowadays, the paper industry plays a very important role in the world economy. The industry is largely based on a raw material that is derived from forest crops with harvest rotations that can approach 100 years in length. The sheer volume of timber required for the industry's production processes is staggering. As shown in **Figure 1–2**[7], about 331 million tons of paper was produced in 2002 worldwide, in which, over 80 million tons of world wide paper is produced in the United States each year, making it the highest paper manufacturer in the world. And then China, Japan, Canada, Germany, Finland, Sweden, France, Korea and Italy are also the prominent paper-producing countries. Among that, the paper production in Japan and China are about 28 and 25 million tons, respectively.

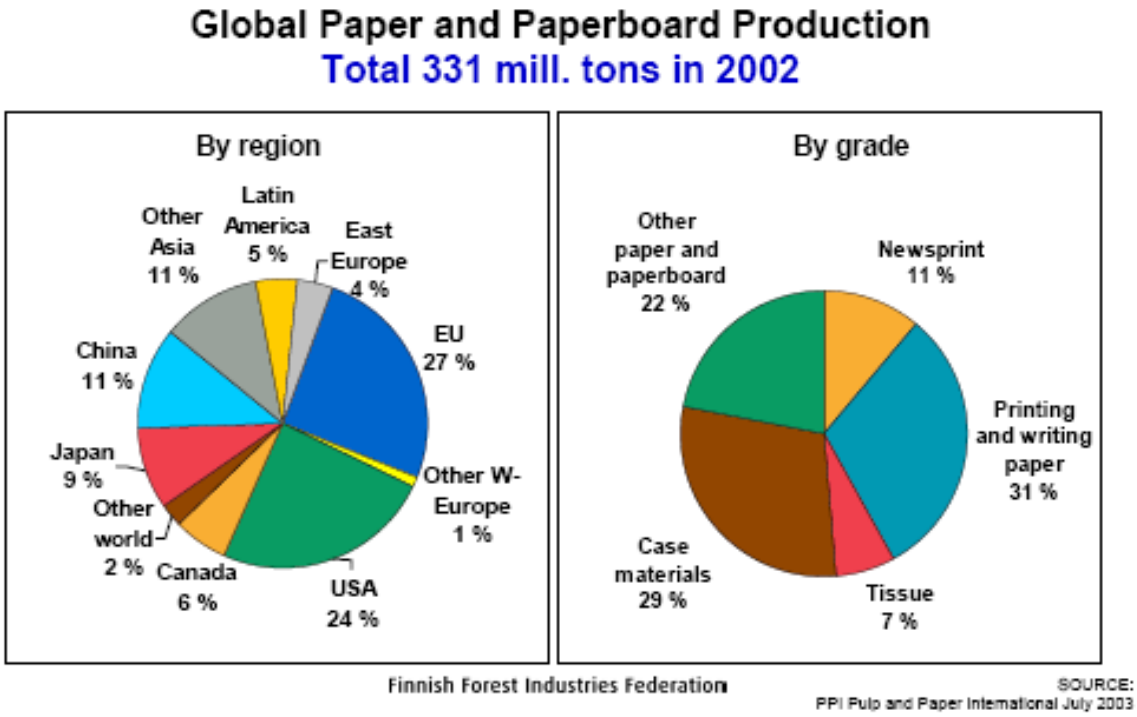


**Figure 1–2 Paper production**

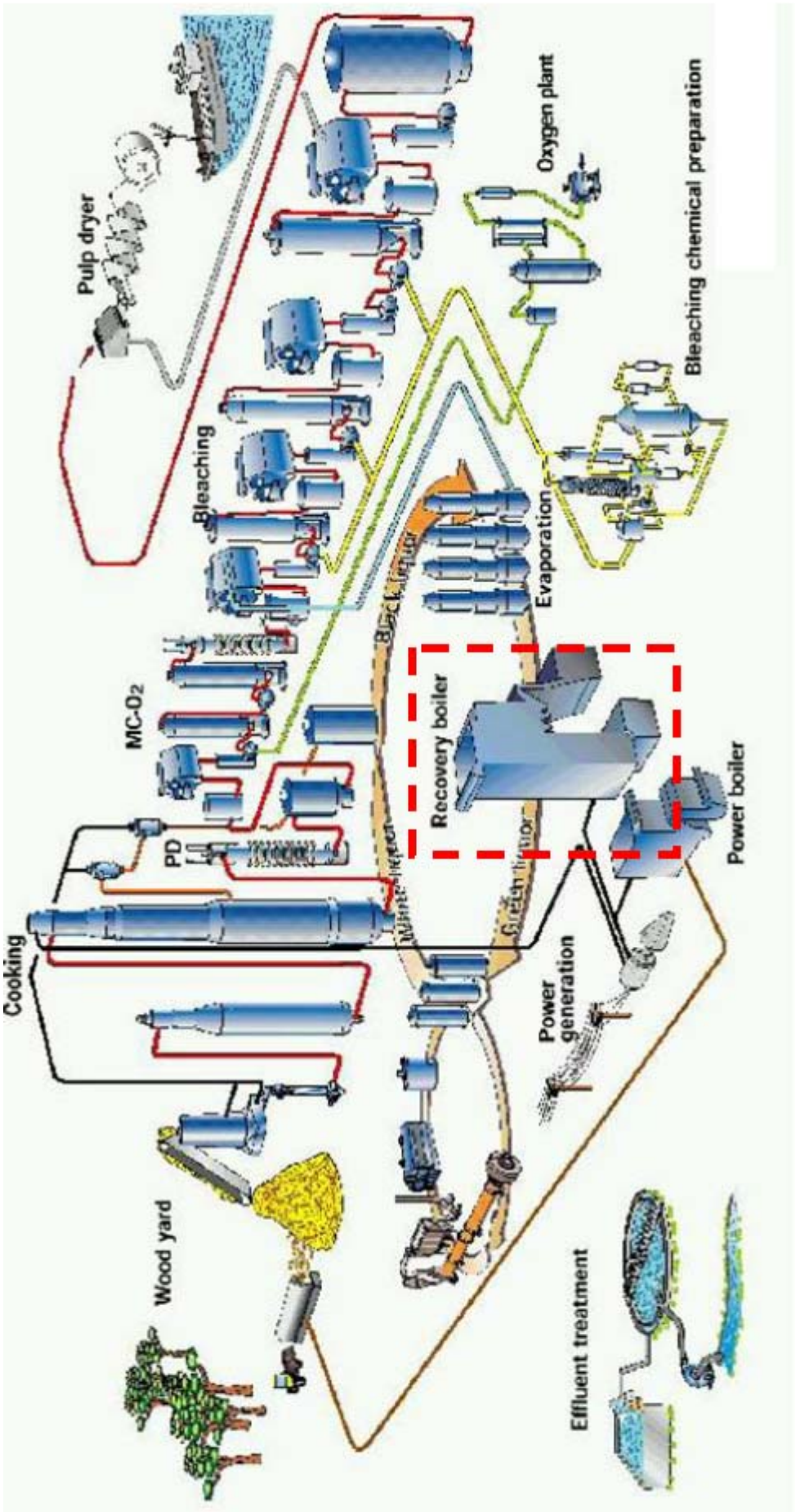


**Figure 1–3 Paper making process**

The dominant route for production of pulp is by a century-old sulfur based chemical process known as “Kraft pulping”, and the paper making process is shown in **Figure 1–3**.[8] The digester is the main process unit and where wood chips are transformed into pulp by cooking at high temperature and pressure in a caustic solution called white liquor (mainly sodium hydroxide and sodium sulfide). The spent cooking liquor exiting the digester, known as black liquor, contains about 15% solids consisting of dissolved organics from the wood and spent pulping chemicals. In a recovery cycle, energy is recovered from the dissolved organic material and the cooking chemicals are regenerated from the intermediary green liquor back to white liquor. Without the recovery cycle, the process would be both economically and environmentally impossible.

### 1.1.2 Black Liquor Production

World-wide, the black liquor production is about 215 million tons dry solids in 2010. The black liquor production keeps a steady increase following the growing demand for pulp paper and is estimated reaching about 270 million tons in 2025. In 2000, the power energy generated from black liquor in Japan was equal to 50 TWh.[9] For example, in Japan, black liquor is utilized for fuel, and 31.5% of fuel energy used in paper mills is provided by black liquor.[8]

### 1.1.3 Utilization of Black Liquor

In comparison with other potential biomass sources for chemicals production, black liquor has great advantage that it is already partially processed and exists in a pumpable and liquid form. In paper mills, there are two basically utilization of black liquor. One is

Tomlinson recovery boiler, and another is black liquor gasification with motor fuels production (BLGMF).

Worldwide, Tomlinson recovery boiler is the most traditional disposal method of black liquor in paper mills.[9] It acts both as a high-pressure steam boiler and as a chemical reactor with reductive and oxidative zones. 2.0 tones of black liquor are produced as a by-product from 1 tone of a hardwood pulp or 1.5 tones of a softwood pulp. Generally, almost all amount of black liquor is used as biomass energy. **Figure 1–4** exhibits the schematic description of the pulping process.[10]

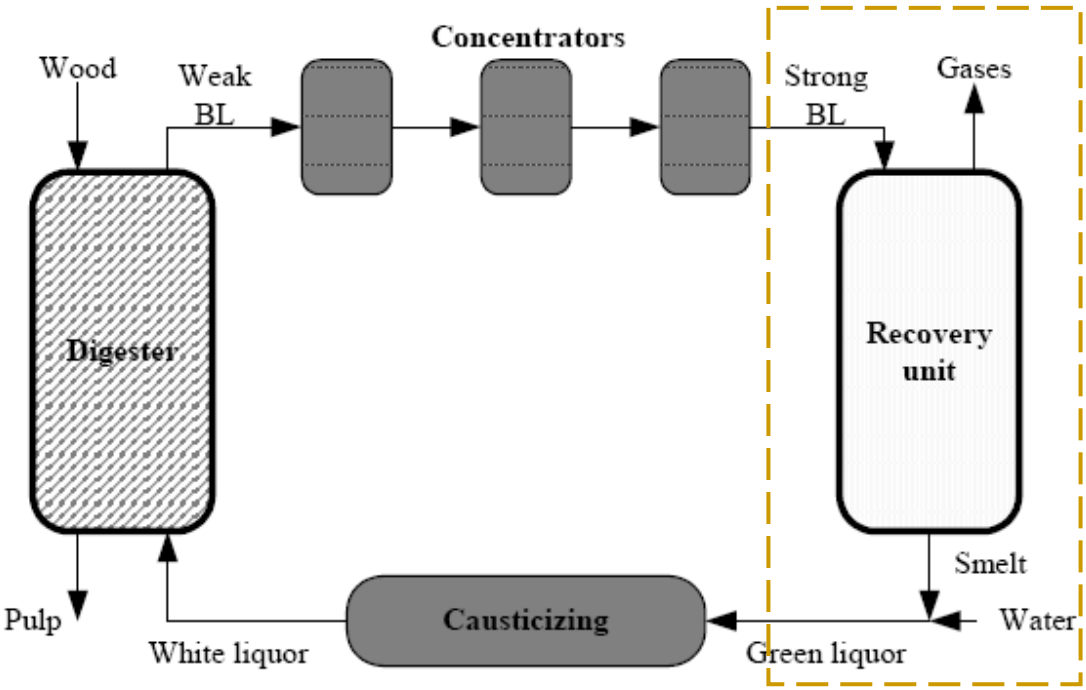


**Figure 1–4 Schematic description of the pulping process**

The weak black liquor has a solid content of approximately 15% by weight, which is far too low for combustion. To raise the solid content in the liquor it is being evaporated by a sequence of concentrators. When the resulting strong black liquor

reaches the recovery boiler, it has a solid content of around 75%. In the recovery unit, black liquor converts some of its chemical energy by full combustion of the liquor which yields an inorganic smelt and gases. Most of the chemicals in the smelt that leaves the recovery unit are then led back into the pulping process as white liquor after causticizing process. A schematic of a Tomlinson recovery boiler can be seen below in **Figure 1–5**.[11]

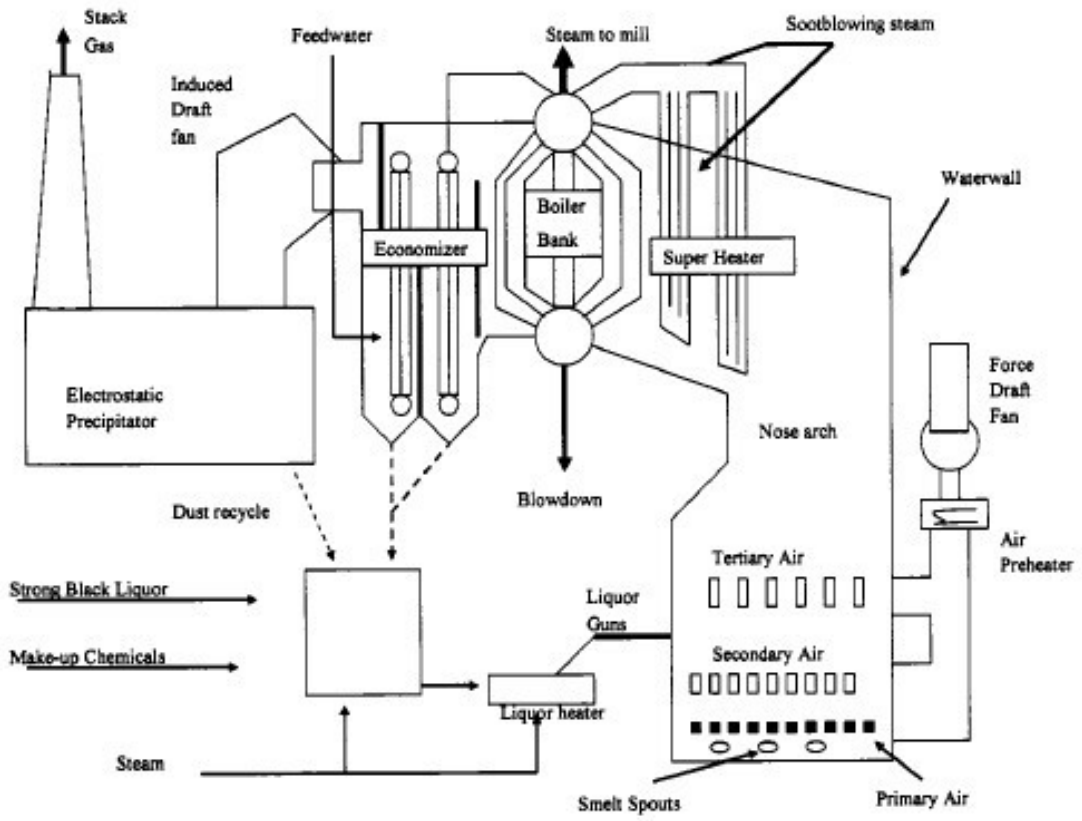


**Figure 1–5 The Tomlinson recovery boiler**

BLGMF is a gasification technology for producing motor fuels, its schematic description is given in **Figure 1–6**.[10] Simply said, the process of burning the black liquor in the recovery boiler producing power and heat in one case is compared with gasification in a gasifier reactor in an alternative case producing methanol or dimethyl

ether (DME).

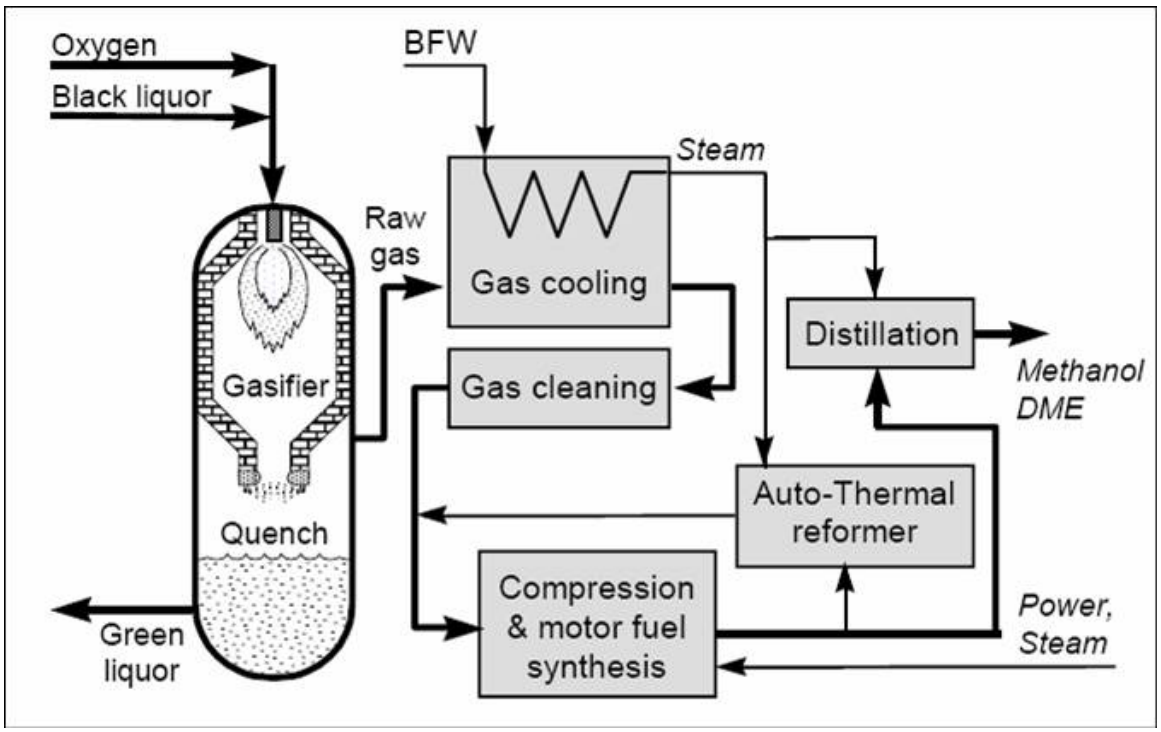


**Figure 1–6 BLGMF system**

The gasifier/quench system of BLGMF is similar to the recovery boiler system in the respect that it converts black liquor into green liquor. But rather than burning the black liquor to form steam, the BLGMF system partially converts the liquor with oxygen to produce a synthesis gas and a molten salt smelt. The synthesis gas is cooled, condensed, compressed and then converted into methanol or alternatively DME in a synthesis reactor.

With this process scheme, almost 70% of the extra biomass energy is transformed to methanol/DME, giving an exergy efficiency about twice that of a recovery boiler system. The methanol/DME output of a black liquor motor fuel system offers the potential to

significantly reduce fossil fuels used for transport.

Although the two methods carry out the partial self-support of energy during the paper making process, they both present such disadvantages: high investment, high operation cost, unstable operation, explosion risk and low energy efficiency (especially for recovery boiler).[12]

In Japan, black liquor is used as fuel energy in paper mill. In 2010, the production of black liquor will reach 70 million tons and the objective of utilization rate is 100%. Black liquor is first evaporated and then transported into recovery boiler. The generated steam is partially used as heat energy, partially used to generate electricity to support the energy demand in the process.

In China, 11,000 paper mills annually discharge black liquor containing 4 million tons of organic material and 1 million tons of alkali, most seriously polluting the environment. Over 95% of the 11,000 paper mills use non-wood raw materials. And generated black liquor is diluted and then discharged directly. The traditional black liquor treatment technology is the traditional alkali recovery technology. Most of the paper mills can not adopt it because it has the disadvantages of high investment, high operation cost, unstable operation, explosion risk, etc. when it's applied to pulping mills using non-wood raw materials.

In general, black liquor keeps a steady increase following the growing demand for pulp paper, but the current recovery methods are high investment and high operation cost, especially for small-scale paper mills. Therefore, develop a low-cost and high efficiency disposal method for utilization of black liquor is necessary.

Black liquor contains about 50% of lignin, which is a good precursor for activated carbon, and the content of Na and K is high, which is effective for the activation process. Until now, few literatures about preparation of porous carbon derived from black liquor has been reported in detail.

### 1.1.4 Previous Studies

The literature gives a report on many works relating to the treatment of black liquor and more particularly of Kraft lignin derived from black liquor.

Demirbaş[5] investigated the pyrolysis and steam gasification processes of black liquor. The result showed that the yields of liquid and gaseous products from pyrolysis of the black liquor samples increase with increasing temperature, and the highest hydrogen rich gas yield was obtained from the catalytic steam gasification run at 1325 K.

Whitty et al.[13] discussed the influence of pressure on pyrolysis of black liquor. It was found that swelling decreased roughly logarithmically over the pressure range 1–20 bar, and the bulk density of the char increased with pressure, indicating that liquors will be entrained less easily at higher pressures.

Cardoso et al.[14] analyzed the effects of black liquor properties on its recovery unit operation. An experimental methodology for characterizing the principal chemical and physical properties of eucalyptus Kraft and bamboo soda black liquors has been developed, and the result showed that eucalyptus and bamboo black liquors present higher contents of non-processing elements (NPEs), higher concentration and different molar mass of lignin than those reported by the pine Kraft black liquor.

Huang et al.[1] investigated aqueous ammonia mixed with caustic potash as wheat straw pulping liquor, and the study provided a new pulping process for wheat straw to reduce problems of discharge black liquor.

Sharma et al.[15] studied the characterization of lignin char and its reactivity towards the formation of polycyclic aromatic hydrocarbons. The result indicated that surface area, presence of inorganics and aromaticity of char may be important factors in polycyclic aromatic hydrocarbon formation. These chars have low reactivity, compared to chars from other biomass constituents, such as chlorogenic acid, pectin and cellulose, probably due to the highly cross-linked and refractory nature of the lignin char.

Xiong et al.[16] developed the application of brown-rot basidiomycete fomitopsis sp. IMER2 for biological treatment of black liquor. This investigation might provide a new idea for treating black liquor using the biological acidification precipitation of brown-rot fungi. Alkali lignin could inhibit the yields of fungal biomass and acid production, but the structure and function of alkali lignin are improved by brown-rot fungus.

Zaied et al.[17] showed that the procedure of electrocoagulation is an effective, fast and economic technique for treatment of black liquor. Under the optimal experimental conditions (initial pH = 7, $t$ = 50 min and $J$ = 14 mA $cm^{-2}$), the treatment of black liquor by electrocoagulation has led to a removal capacity of 98% of COD, 92% of polyphenols and 99% of color intensity with a good repeatability (R.S.D.< 3%).

High surface area activated carbons (ACs) were prepared from lignin precipitated from kraft black liquor by Gonzalez-Serrano et al.[18] using chemical activation by $ZnCl_2$. It was suggested that ACs with a porous structure suitable for gas phase applications

could be prepared using a temperature as low as 400 $^{o}$C. Although these authors obtained good materials from lignin, it should be pointed out that the use of $ZnCl_2$ is nowadays not recommended due to the toxicity of zinc.

Gnonzalez-Serrano et al.[19] also prepared ACs from $H_3PO_4$ activation of lignin from kraft black liquors. An impregnation ratio and an activation temperature around 2 g $H_3PO_4$/g lignin and 700 K, respectively, are recommended as the best combination of operating conditions to prepare ACs with a high BET surface area and a well developed porosity for aqueous phase applications.

Fierro et al.[20] prepared ACs from kraft lignin from black liquor by chemical activation using $H_3PO_4$. Various parameters like effect of impregnation ratio (acid/lignin = 0.7–1.75), carbonization temperature (400–650 $^{o}$C) and impregnation time (1–48 h) were studied. It was suggested the optimum temperature for porosity development in lignin-derived ACs was 600 $^{o}$C. Furthermore, they suggested that the acid/lignin ratio strongly affects the pore structure and char yield, and the effect of impregnation time is more important at high carbonization temperature due to decomposition of phosphate and polyphosphate bridges cross-linking parts of the carbon structure.

## 1.2 Electric Double Layer Capacitor (EDLC)

EDLC is an electrochemical capacitor that has an unusually high energy density when compared to common capacitors, typically on the order of thousands of times greater than a high capacity electrolytic capacitor.[21–23] EDLCs have attracted worldwide research interest because of the variety of commercial applications as energy storage

devices in many fields, notably in "energy smoothing" and momentary-load devices.[24–25] They have applications as energy-storage devices used in vehicles and for smaller applications like home solar energy systems where extremely fast charging is a valuable feature.

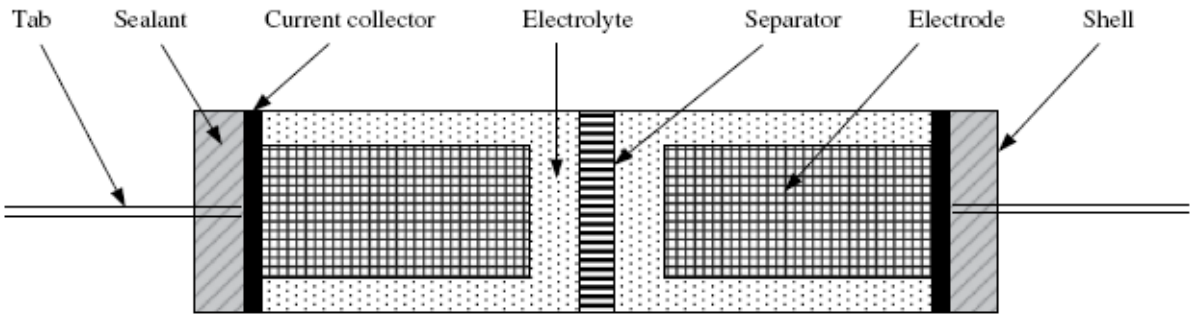


**Figure 1–7 Basic structure model of EDLCs**

The charge-storage mechanism of EDLC is predominately due to double-layer charging effects. But in general, additional contributions of pseudo capacitance may also be part of the observed capacitance due to the functional groups present on the electrode surface.[26] EDLC is similar to a battery, they both require two electrodes (anode and cathode), an electrolyte, and a conducting charge path in order to operate. EDLCs also have an additional component, the separator that electrically isolates the two electrodes. These four components are then packaged together and can be used as a conventional capacitor would be, where the main structural difference is that in most EDLCs both the positive and negative electrodes are made of the same material. EDLCs are comprised of many individual cells (parallel or serial) in series to have high capacitance and work voltage. **Figure 1–7**[27] and **Figure 1–8**[28] depict the typical structure model and principle

of EDLCs, respectively.

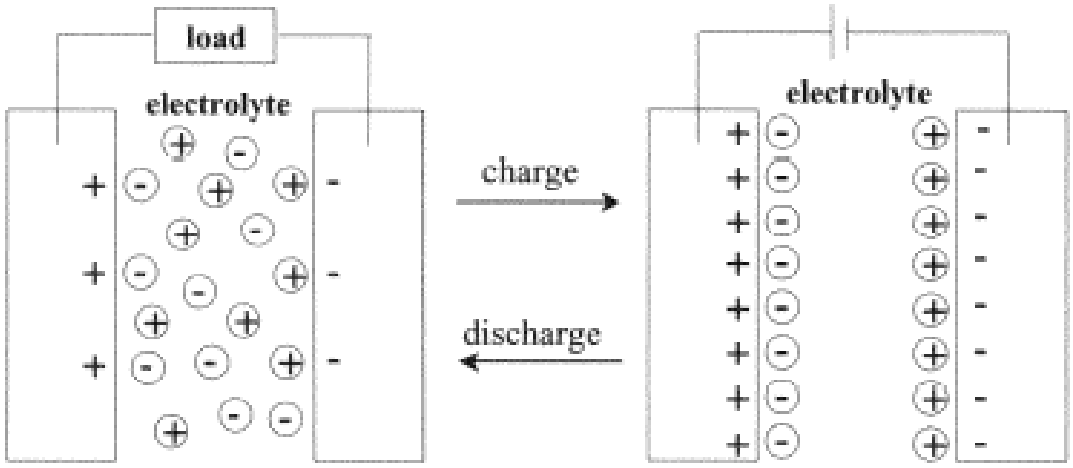


**Figure1–8 Principle of an EDLC**

## 1.2.1 Electrolyte Solution

A majority of commercial EDLCs use non-aqueous electrolyte solutions to achieve high terminal voltage, $V$, because the capacitor energy, $E$, and the maximum power, $P_{max}$, are given by

$$E = CV^2/2 \quad \text{and} \quad P_{\max} = V^2/4R$$

Where $C$ is the cell capacitance in F and $R$ is the internal resistance in Ω.[29] The EDLCs using non-aqueous electrolyte solutions dominate the market for capacitors focusing on energy storage, but those using aqueous electrolyte solutions are also marketed. Aqueous solutions are potentially beneficial to large installations for storage of surplus power and unsteady electricity generated by natural energy resources, because of low cost, high

safety, long lifetime and low internal resistance. Representative electrolytes are listed in **Table 1–1**, where some properties are also indicated.[30]

**Table 1–1 Common used electrolytes**

| Electrolytes | Ion size (nm) | |
|---|---|---|
| | Cation | Anion |
| Organic electrolytes | | |
| $(C_2H_5)_4N{\cdot}BF_4$ ($TEA^+BF_4^-$) | 0.686 | 0.458 |
| $(C_2H_5)_3(CH_3)N{\cdot}BF_4$ ($TEMA^+BF_4^-$) | 0.654 | 0.458 |
| $(C_2H_5)_4P{\cdot}BF_4$ ($TEP^+BF_4^-$) | | 0.458 |
| $(C_4H_9)_4N{\cdot}BF_4$ ($TBA^+BF_4^-$) | 0.830 | 0.458 |
| $(C_6H_{13})_4N{\cdot}BF_4$ ($THA^+BF_4^-$) | 0.96 | 0.458 |
| $(C_2H_5)_4N{\cdot}CF_3SO_3$ | 0.686 | 0.540 |
| $(C_2H_5)_4N{\cdot}(CF_3SO_2)_2N$ ($TEA^+TFSI^-$) | 0.68 | 0.650 |
| Inorganic electrolytes | | |
| $H_2SO_4$ | | 0.533 |
| KOH | 0.26 | |
| $Na_2SO_4$ | 0.36 | 0.533 |
| NaCl | 0.36 | |
| $Li{\cdot}PF_6$ | 0.152 | 0.508 |
| $Li{\cdot}ClO_4$ | 0.152 | 0.474 |

## 1.2.2 Comparison of EDLC and Batteries

The EDLCs are superior to lithium ion batteries (LIBs) because of high power density (discharge at high current density), short time needed for full charging, long cycle

life (no chemical reactions), high coulombic efficiency (high reversibility), and environmental friendliness (no heavy metals used), even though their energy density is lower than LIBs.[31–34] In addition, the positive electrode of LIB requires certain amounts of cobalt ions, which is one of the rare metals, whereas carbon is inexhaustible.

Differences between LIB and EDLC are originated from their storage mechanisms of electricity: faradaic intercalation/deintercalation reactions of lithium ions on both electrodes, positive electrode of $LiMO_2$ (M: Co, Ni, Mn, etc.) and negative electrode of graphite in LIB, but physical adsorption/desorption of electrolyte ions on both electrodes in EDLC.[29] As a consequence, relatively high power density can be obtained, but energy density is relatively low, but charge/discharge rate and efficiency can be high in EDLCs.

The capacitance of EDLCs is proportional to the effective surface area of electrode and a dielectric constant, and is inversely proportional to the thickness of EDLCs. The surface area of the electrodes is a crucial factor to increase capacitance, so that ACs with a large surface area are employed as electrodes, in addition to fairly good electric conductivity, electrochemical inertness, and lightweight properties of carbon materials.

As advantages described above, EDLCs using ACs are now set in various electronic devices and instruments, such as the backup power sources in the copy machines, the power boosters for forklifts, cranes and heavy construction-equipments, and the street lamps and signals in combination with solar panels. The EDLCs have been used for hybrid buses and trucks, but installation to electric vehicle driveline as a main power source is thought to be difficult because of their low energy density, but there are still many efforts to get high energy density.

### 1.2.3 Previous Studies

In last decades, a number of reviews and articles on carbon materials related to EDLCs have been published.

Qiao et al.[35] prepared high-performance EDLC from ACs using needle coke by KOH activation. AS-prepared ACs exhibit large surface areas (400–2900 $m^2\ g^{-1}$), high EDLC capacitances (14–44 F $g^{-1}$), and low system resistances (8.3–18.7 Ω) on the basis of the anisotropic texture of their precursor.

Lozano-Castelló et al.[36] investigated the influence of pore structure and surface chemistry on electric double layer capacitance in non-aqueous electrolyte. The results showed that, in general, capacitance increases with surface area. However, the results confirm that capacitance not only depends on surface area, but also on two other parameters: pore size distribution and surface chemistry. They prepared a KOH-AC with a capacitance as high as 220 F $g^{-1}$. Finally, the results obtained with a mesoporous sample showed that the presence of mesopores in ACs with very high surface area (e.g. > 2000 $m^2\ g^{-1}$), do not seem to be effective for double layer capacitors.

Kim et al.[37] chose a mesophase pitch-based carbon fiber (MPCF) and an isotropic pitch-based carbon fiber (IPCF) with different microstructures for EDLCs. The results suggested that the MF-series prepared from MPCFs by several KOH fractions exhibited a good capacitance in comparison with the IF-series prepared from IPCFs, although the former had smaller specific surface areas than those of the latter. The specific capacitance per weight (F $g^{-1}$) of both samples increased with an increase in KOH fraction. Further evaluation of the capacitance using the specific capacitance per unit area elucidates the

efficiency of the surface area.

Barbieri et al.[38] used a large specific surface area of carbon materials for EDLC. They suggested that the limitation of gravimetric capacitance can be ascribed to a space constriction for charge accommodation inside the pore walls. As a consequence, the use of extremely high surface area carbons for EDLCs may be unprofitable.

Xu et al.[39] investigated the competitive effects on the performance of the EDLCs between porosity increase and simultaneous conductivity decrease for KOH-activated carbon nanotubes. It was found that the KOH activation enhances the specific surface area of carbon nanotubes and its specific capacitances but decreases its electric conductivity and the rate performance in EDLC.

## 1.3 Activated Carbon

AC is widely used in the adsorption of gases, liquids and solids because of its high surface area.[40–42] The methods of manufacturing AC include the physical and chemical methods.[43] The physical method requires two steps: carbonizing organic material at high temperature in an inert atmosphere, following by a treatment of the carbon with $CO_2$ or steam, or their mixture. The chemical method involves heating the mixture of organic material and active agents at high temperature, then rinsing the active agents and drying the carbon.

The pores of ACs are classified in three groups: micropores (diameter $d<2$ nm), mesopores ($2\ nm<d<50$ nm) and macropores ($d>50$ nm).[44] The micropores constitute the largest part of the internal surface and are accessible to the adsorptive molecules.

Generally, micropores contribute at least 90% of the total surface area of an AC. The mesopores contribute significantly to adsorption because of capillary condensation. Mesopores also can adsorb many macromolecules and ions larger than the pore diameter of micropores for the adsorbate. Acs with different pore structures and pore distribution are used for a variety of different applications.

### 1.3.1 Waste Material Precursor

AC can be manufactured from several materials, such as wood, coal and some polymers. Wood and coal are relatively economical, but polymers are the main source of pure carbon. Due to the high production costs, now waste materials are used for preparation of ACs. AC production costs can be reduced by either choosing a cheap raw material or by applying a proper production method[45]; nevertheless, it is still a challenge to prepare AC with very specific characteristics, such as a given pore size distribution, and using low-cost raw materials processed at low temperature (less energy costs).[40]

Therefore, it is necessary to find suitable low-cost raw materials that are economically attractive and at the same time present similar or even better characteristics than the conventional ones. The use of waste materials for the preparation of AC is very attractive from the point of view of their contribution to decrease the costs of waste disposal, therefore helping environmental protection.[46]

### 1.3.2 ACs as Electrodes

Metal oxides, conducting polymers and carbons are the main electrode materials for EDLCs.[28] Among which, carbon materials for electrochemical energy devices, such as

secondary batteries[47], fuel cells[48], and supercapacitors[49], have been extensively studied. However, each type of electrochemical energy device requires different physical properties and morphology. For supercapacitors, the carbon material for the EDLC type must have high specific surface area, good intra- and interparticle conductivity in porous matrices, good electrolyte accessibility to intrapore surface area, and the available electrode production technologies.[36–37]

ACs are much cheaper than metal oxides and conducting polymers and they have much larger specific surface area than the others. AC-based supercapacitors have been commercialized for small memory backup devices. During the last decades, the application of ACs as the electrode materials in supercapacitors has been intensively investigated because of their high specific surface area and relatively low cost. Theoretically, the higher the specific surface area of an AC, the higher the specific capacitance should be expected. Practically, the situation is more complicated, some ACs with smaller surface area give a larger specific capacitance than those with a larger surface area, because a significant part of the surface area remains in the micropores, which are not accessible to the electrolyte ions.[36] Therefore, the pore size distribution together with the surface area is important for the determination of capacitance.

### 1.3.3 Previous Studies

Qian et al.[50] prepared ACs from cattle-manure compost by $ZnCl_2$ activation, and the influence of activation parameters such as impregnation ratio, activation temperature and retention time on the final products was investigated. The results showed that the surface

area and pore volume of ACs were achieved as high as 2170 $m^2$ $g^{-1}$ and 1.70 $cm^3$ $g^{-1}$, respectively.

Hu et al.[51] also prepared high surface area ACs from coconut shell with KOH activation, and the influences of KOH to shell ratio, activation temperature and pre-heat temperature were investigated. AC with the BET surface area and pore volume as high as 2451 $m^2$ $g^{-1}$ and 1.21 $cm^3$ $g^{-1}$ was obtained. Besides, the ACs exhibited a much higher adsorption capacity for phenol, 4-chlorophenol and 4-nitrophenol from aqueous solution than did a commercial AC.

Roh et al.[52] synthesized low surface area ACs using multi-step activation for use in EDLC. The specific capacitance of the ACs heat treated at between 650 and 900 $^oC$ was increased up to 118 F $ml^{-1}$, even with a low surface area carbon (< 50 $m^2$ $g^{-1}$).

Li et al.[53] prepared a series of ACs with the specific surface area between 1330 and 1510 $m^2$ $g^{-1}$ from starch for electrochemical capacitors. The ACs showed excellent electric performance with the high specific capacitance between 170 and 220 F $g^{-1}$.

Mitani et al.[54] activated raw pitch coke with alkali hydroxide at 500–900 $^oC$ to prepare high performance carbon for EDLC. It was found that the high surface area provided by KOH led to a high capacitance per weight of 39 F $g^{-1}$. However, its capacitance per volume was as low as 16 F $ml^{-1}$. Although the coke of moderate surface area showed a similar capacitance per weight, its capacity per volume was as high as 28 F $ml^{-1}$ because of its high density. The authors suggested that adequate porosity must be selectively introduced by NaOH activation to the coke to obtain moderate surface area. Much smaller expansion of layers in the present needle type coke activated by NaOH

than that by KOH is indicative for the higher density of the former activated coke.

## 1.4 Objective of This Study

Nowadays, black liquor keeps a steady increase following the growing demand for pulp paper. Although the current recovery methods carry out the partial self-support of energy during the paper making process, they both present such disadvantages: high investment, high operation cost, unstable operation, explosion risk and low energy efficiency (especially for recovery boiler). Therefore, develop a low-cost and high efficiency disposal method for utilization of black liquor is urgent. As black liquor is rich in the content of alkali compounds, it could be a good precursor for preparing ACs. Besides, ACs with a large surface area are employed as electrodes, in addition to fairly good electric conductivity, electrochemical inertness, and lightweight properties of carbon materials. So the objective of this study is to prepare EDLC from ACs derived from black liquor to carry out the high value utilization of black liquor, but to some extent, no literature about preparation of EDLC from porous carbon derived from black liquor has been reported in detail. This study will achieve such advantages as follows:

(1) Low operation cost

(2) Environmentally friendly

(3) Porous and low-cost ACs

(4) High surface area ACs

(5) Good capacitive performance

(6) Economizing the amount of activating agent

## 1.5 References


(1) Huang G.L.; Shi, J.X.; Langrish, T.A.G. A new pulping process for wheat straw to reduce problems with the discharge of black liquor. *Bioresour. Techenol.* **2007**, *98*(15), 2829–2835.

(2) McKeough, P. Research on black–liquor conversion at the technical research centre of Finland. *Bioresour. Techenol.* **1993**, *46*(1–2), 135–143.

(3) González, C.; Alvarez, R.; Coca, J. Use of kraft black liquors from a pulp mill for the production of soil conditioners. *Waste Manage. Res.* **1992**, *10*(2), 195–201.

(4) Sricharoenchaikul, V. Assessment of black liquor gasification in supercritical water. *Bioresour. Techenol.* **2009**, *100(2)*, 638–643.

(5) Demirbaş, A. Pyrolysis and steam gasification processes of black liquor. *Energy Convers. Manage.* **2002**, *43*(7), 877–884.

(6) Yokoyama, S. The Asian Biomass Handbook–A guide for biomass production and utilization. The Japan Institute of Energy. *http://aba.jie.or.jp/aba_handbook.htm*

(7) World wide paper & pulp supply website. *http://individual.utoronto.ca/abdel_rahman/paper/index.html*

(8) Ekbom T, Berglin N, Lögdberg S. High efficient motor fuel production from biomass via black liquor gasification. In: Proceedings of the 15th international symposium on alcohol fuels, San Diego, USA; September 26–28, **2005**.

(9) Kohl, A.L. Black liquor gasification. *Can. J. Chem. Eng.* **1986**, *64*(4), 299–304.

(10) Marklund, M. Black liquor recovery: how does it work? Energy Technology Center,

Sweden, *http://www.etcpitea.se/blg/document/PBLG_or_RB.pdf*

(11) Connolly, T.S. $CO_2$ pyrolysis and gasification of krafe black liquor char. Ph.D thesis. The university of maine. **2006**.

(12) Puértolas, R.; Gea, G.; Murillo, M.B.; Arauzo, J. Pyrolysis of black liquors from alkaline pulping of straw. Influence of a preoxidation stage on the char characteristics. *J. Anal. Appl. Pyrolysis* **2001**, *58–59*, 955–966.

(13) Whitty, K.; Backman, R.; Hupa, M. Influence of pressure on pyrolysis of black liquor: 1. Swelling. *Bioresour. Techenol.* **2008**, *99*(3), 663–670.

(14) Cardoso, M.; Oliverira, É.D.; Passos, M.L. Chemical composition and physical properties of black liquors and their effects on liquor recovery operation in Brazilian pulp mills. *Fuel* **2009**, 88(4), 756–763.

(15) Sharma, R.K.; Wooten, J.B.; Baliga, V.L.; Lin, X.H.; Chan, W.G.; Hajaligol, M.R. Characterization of chars from pyrolysis of lignin. *Fuel* **2004**, 83(11–12), 1469–1482.

(16) Xiong, Z.; Zhang, X.Y.; Wang, H.X.; Ma, F.Y.; Li, L.; Li, W. Application of brown-rot basidiomycete fomitopsis sp. IMER2 for biological treatment of black liquor. *J. Biosci. Bioeng.* **2007**, 104(6), 446–450.

(17) Zaied, M.; Bellakhal, N. Electrocoagulation treatment of black liquor from paper industry. *J. Hazard. Mater.* **2009**, *163*(2–3), 995–1000.

(18) Gonzalez-Serrano, E.; Cordero, T.; Rodriguez-Mirasol, J.; Cotoruelo, L.; Rodriguez, J.J. Removal of water pollutants with activated carbons prepared from $H_3PO_4$ activation of lignin from kraft black liquors. *Water Res.* **2004**, *38*(13), 3043–3050.

(19) Gonzalez-Serrano, E.; Cordero, T.; Rodríguez-Mirasol, J.; Rodríguez, J.J. Development of porosity upon chemical activation of kraft lignin with $ZnCl_2$. *Ind. Eng. Chem. Res.* **1997**, *36*(11), 4832–4838.

(20) Montané, D.; Torné-Fernández, V.; Fierro, V. Activated carbons from lignin: kinetic modeling of the pyrolysis of Kraft lignin activated with phosphoric acid. *Chem. Eng. J.* **2005**, *106*(1), 1–12.

(21) Frackowiak, E.; Béguin, F. Carbon materials for the electrochemical storage of energy in capacitors. *Carbon* **2001**, *39*(6), 937–950.

(22) Conway, B.E.Transition from 'supercapacitor' to 'battery' behavior in electro-chemical energy storage. *J. Electrochem. Soc.* **1991**, *138*(6), 1539–1548.

(23) Sarangapani, S.; Tilak, B.V.; Chen, C.P. Materials for electrochemical capacitors. *J. Electrochem. Soc.* **1996**, *143*(11), 3791–3799.

(24) Lewandowski, A.; Galinski, M. Practical and theoretical limits for electrochemical double–layer capacitors. *J. Power Sources* **2007**, *173*(2), 822–828.

(25) Bohlen, O.; Kowal, J.; Sauer, D.U. Ageing behaviour of electrochemical double layer capacitors: Part I. Experimental study and ageing model. *J. Power Sources* **2007**, *172*(1), 468–475.

(26) Mitra, S.; Sampath, S. Electrochemical capacitors based on exfoliated graphite electrodes. *Electrochem. Solid–State Lett.* **2004**, *7*(9), A264–268.

(27) Zhang, Y.; Feng, H.; Wu, X.B.; Wang, L.Z.; Zhang, A.Q.; Xia, T.C.; Dong, H.C.; Li, X.F.; Zhang, L.S. Progress of electrochemical capacitor electrode materials: A review. *Int. J. Hydrogen Energy* **2009**, *34*(11), 4889–4899.

(28) Lee, Y.H.; An, K.H.; Lee, J.Y.; Lim, S.C. Carbon nanotube–based supercapacitors. *Encyclopedia of Nanoscience and Nanotechnology* **2004**, *1*, 625–634.

(29) Inagaki, M.; Konno, H.; Tanaike, O. Carbon materials for electrochemical capacitors. *J. Power Sources* **2010**, *195*(24), 7880–7903.

(30) Ue, M. Mobility and ionic association of lithium and quaternary ammonium salts in propylene carbonate and γ–butyrolactone. *J. Electrochem. Soc.* **1994**, *141*(12), 3336–3342

(31) Yoshida, A.; Nonaka, S.; Aoki, I.; Nishino, A. Electric double–layer capacitors with sheet–type polarizable electrodes and application of the capacitors. *J. Power Sources* **1996**, *60*(2), 213–218.

(32) Kibi, Y.; Saito, T.; Kurata, M.; Tabuchi, J.; Ochi, A. Influence of physical properties of activated carbons on characteristics of electric double–layer capacitors. *J. Power Sources* **1996**, *60*(2), 225–231.

(33) Kötz, Y.; Carlen, M. Principles and applications of electrochemical capacitors. *Electrochim. Acta* **2000**, *45*(15–16), 2483–2498.

(34) Endo, M.; Takeda, T.; Kim, Y.J.; Koshiba, K.; Ishii, K. High power electric double layer capacitor (EDLC's); from operating principle to pore size control in advanced carbons. *Carbon Sci.* **2001**, *1*(3–4), 117–128.

(35) Qiao, W.M.; Yoon, S.H.; Mochida, I. KOH activation of needle coke to develop activated carbons for high–performance EDLC. *Energy Fuels* **2006**, *20*(4), 1680–1684.

(36) Lozano-Castelló, D.; Cazorla-Amorós, D.; Linares-Solano, A.; Shiraishi, S.;

Kurihara, H.; Oya, A. Influence of pore structure and surface chemistry on electric double layer capacitance in non–aqueous electrolyte. *Carbon* **2003**, *41*(9), 1765–1775.

(37) Kim, Y.J.; Horie, Y.; Matsuzawa, Y.; Ozaki, S.; Eindo, M.; Dresselhaus, M.S. Structural features necessary to obtain a high specific capacitance in electric double layer capacitors. *Carbon* **2004**, *42*(12–13), 2423–2432.

(38) Barbier, O.; Hahn, M.; Herzog, A.; Kötz, R. Capacitance limits of high surface area activated carbons for double layer capacitors. *Carbon* **2005**, *43*(6), 1303–1310.

(39) Xu B.; Wu, F.; Su, Y.F.; Cao, G.P.; Chen, S.; Zhou, Z.M.; Yang, Y.S. Competitive effect of KOH activation on the electrochemical performances of carbon nanotubes for EDLC: Balance between porosity and conductivity. *Electrochim. Acta* **2008**, *53*(26), 7730–7735.

(40) Sudaryanto, Y.; Hartono, S.B.; Irawaty, W.; Hindarso, H.; Ismadji, S. High surface area activated carbon prepared from cassava peel by chemical activation. *Bioresour. Techenol.* **2006**, *97*(5), 734–739.

(41) Suzuki, R.M.; Andrade, A.D.; Sousa, J.C.; Rollemberg, M.C. Preparation and characterization of activated carbon from rice bran. *Bioresour. Techenol.* **2007**, *98*(10), 1985–1991.

(42) Hayashi, J. Kazehaya, A.; Muroyama, K.; Watkinson, A.P. Preparation of activated carbon from lignin by chemical activation. *Carbon*, **2000**, *38*(13), 1873–1878.

(43) Suhas; Carrott, P.J.M.; Ribeiro Carrott, M.M.L. Lignin–from natural adsorbent to activated carbon: a review. *Bioresour. Techenol.* **2007**, *98*(12), 2301–2312.

(44) Moreno-Castilla, C. Adsorption of organic molecules from aqueous solutions on carbon material. *Carbon* **2004**, *42*(1), 83–94.

(45) Lafi, W.K. Production of activated carbon from acorns and olive seeds. *Biomass Bioenergy* **2001**, *20*(1), 57–62.

(46) Dias, J.M.; Alivim-Ferraz, M.C.M.; Almeida, M.F.; Rovera-Utrolla, J.; Sánchez-Polo, M. Waste materials for activated carbon preparation and its use in aqueous–phase treatment: a review. *J. Environ. Manage.* **2007**, *85*(4), 833–846.

(47) Sato, Y.; Tanuma, K.; Takayama, T.; Kobayakawa, K.; Kawai, T.; Yokoyama, A. $^{7}$Li–nuclear magnetic resonance observations of lithium insertion into coke carbon modified with mesophase–pitch. *J. Power Sources* **2001**, *97–98*, 165–170.

(48) Wang, X.; Hsing, I.M.; Yue, P.L. Electrochemical characterization of binary carbon supported electrode in polymer electrolyte fuel cells. *J. Power Sources* **2001**, *96*(2), 282–287.

(49) Gamby, J.; Taberna, P.L.; Simon, P.; Fauvarque, J.F.; Chesneau, M. Studies and characterisations of various activated carbons used for carbon/carbon supercapacitors. *J. Power Sources* **2001**, *101*(1), 109–116.

(50) Qian, Q.R.; Machida, M.; Tatsumoto, H. Preparation of activated carbons from cattle–manure compost by zinc chloride activation. *Bioresour. Techenol.* **2007**, *98*(2), 353–360.

(51) Hu, Z.H.; Srinivasan, M.P. Preparation of high–surface–area activated carbons from coconut shell. *Microporous Mesoporous Mater.* **1999**, *27*(1), 11–18.

(52) Roh, K.C.; Park, J.B.; Lee, C.T.; Park, C.W. Study on synthesis of low surface area

activated carbons using multi–step activation for use in electric double layer capacitor. *J. Ind. Eng. Chem.* **2008**, *14*(2), 247–251.

(53) Li, Q.Y.; Wang, H.Q.; Dai, Q.F.; Yang, J.H.; Zhong, Y.L. Novel activated carbons as electrode materials for electrochemical capacitors from a series of starch. *Solid State Ionics* **2008**, *179*(7–8), 269–273.

(54) Mitani, S.; Lee, S.I.; Yoon, S.H.; Korai, Y.; Mochida, I. Activation of raw pitch coke with alkali hydroxide to prepare high performance carbon for electric double layer capacitor. *J. Power Sources* **2004**, *133(*2), 298–301.

# Chapter 2 Preparation and Characterization of ACs from Black Liquor

## 2.1 Introduction

ACs are known as very effective adsorbents due to their highly developed porosity, large surface area (that can reach 3000 $m^2$ $g^{-1}$), variable characteristics of surface chemistry, and high degree of surface reactivity.[1–2] These unique characteristics make AC very versatile materials, which have been studied not only as adsorbents,[3–4] but also as catalysts and electrode materials.[5–6] ACs can be prepared from a large number of materials, such as wood, coal, lignite etc.[7] Due to the increasing demand of ACs, low-cost precursors are urgently in demand.

Black liquor is the waste from the production of papermaking fibers via the alkaline kraft process (sulfate method). Nowadays, black liquor is an important industrial fuel in papermaking countries.[8] A certain amount of work has already been carried out on the production of ACs from lignin derived from black liquor. Hayashi et al.[9] prepared ACs from lignin by chemical activation with $ZnCl_2$, $H_3PO_4$ and some alkali metal compounds. The results showed that AC with a surface area of nearly 2000 $m^2$ $g^{-1}$ was obtained from $K_2CO_3$ activation. Gonzalez-Serrano et al.[10] showed that ACs with a high BET surface area and a well-developed porosity have been prepared from pyrolysis of $H_3PO_4$-impregnated lignin. Although lignin is an interesting precursor for ACs, it presents the

disadvantage of being expensive because of its recycling cost. Black liquor contains about 50% of lignin along with high content of alkali metals (Na, K, etc.),[8, 11] which are effectively used to improve the activation process.[12] Therefore, preparation of ACs directly from black liquor may reduce the cost not only for lignin-recycling but also for activating agents, but to some extent, scarcely any research was reported, and the influence of alkali metals exist in black liquor on activation was examined for the first time in our study.

In this chapter, the preparation of ACs from black liquor was carried out by chemical activation with alkali compounds. The influence of preparation conditions (carbonization temperature, activation temperature, holding time and the weight ratio of activating agent/char) on the pore structure of ACs was taken into account. Besides, the activation effect of ACs prepared from char and eluted char was compared to testify if the alkali metals exist in black liquor react as activating agent in the process of activation.

## 2.2 Experimental

### 2.2.1 Sample

Black liquor used in this study as a starting material was obtained from Mitsubishi Corporation, Japan. **Figure 2–1** shows the shape of black liquor sample. An ultimate analysis was conducted with a Leco CHN-2000 elemental determinator and a Leco SC-432 sulfur determinator (Leco Corp., St. Joseph, MI). Quantitative analysis of Na and K was carried on an ICA-2000 ion chromatography (TOADKK, Japan). **Table 2–1**

summarizes the main characteristics of the black liquor sample. According to **Table 2–1**, the moisture content of black liquor is as high as 83.3%, since the sample was not concentrated. It is the weak black liquor without evaporation. Otherwise, the ash content is also high, due to the alkali compounds existing in black liquor.


**Figure 2–1 Black liquor sample**

## 2.2.2 Thermogravimetric Analysis

The weight loss behavior of black liquor was performed on a TGD9600S analyzer (ULBAC-RIKO, Japan). Black liquor after vacuum drying of about 7 mg was heated from room temperature to 1000 $^{o}$C at a heating rate of 10 $^{o}$C/min under Ar flow, and then the thermo gravimetric (TG) plots of black liquor was obtained.

## 2.2.3 Carbonization Process

Black liquor was put in four crucibles (size: Ø60 × H70 mm) and then put inside a crucible case (size: L150 × W150 × H70 mm). Afterward the sample was carbonized in muffle (FUW230PA, Toyo, Japan) under Ar flow (2 L/min). The carbonization condition

was as follows: hold for 30 min at room temperature to drive the air away, and then heated up from room temperature to the final temperature (500–900 $^{o}$C) with the heating rate of 10 $^{o}$C/min, and then held for 2 h at the final temperature. After carbonization, the char sample was obtained, and the char yield was calculated.

**Table 2–1 Proximate and ultimate analyses (wt.%) of Black liquor**

| Proximate analysis | Black liquor |
|---|---|
| Moisture [wt.%] | 83.3 |
| Ash [wt.%, dry] | 40.7 |
| Volatile matter [wt.%, dry] | 41.0 |
| Fixed carbon [wt.%, dry] | 18.3 |
| Ultimate analysis (wt.%, daf) | |
| C | 59.4 |
| H | 5.3 |
| N | 0.2 |
| S | 5.7 |
| O (by difference) | 29.4 |
| Na [mg/g, as received] | 32.1 |
| K [mg/g, as received] | 3.0 |

## 2.2.4 Activation Process

The char sample was pulverized to pass through a 150 mesh sieve (<106 μm). Moreover, the char sample of approximately 2–4 g was put in a crucible, and thermally treated under continuous Ar flow in an electrically heated horizontal tube furnace (size:

Ø50×L600 mm, shown in **Figure 2–2**).

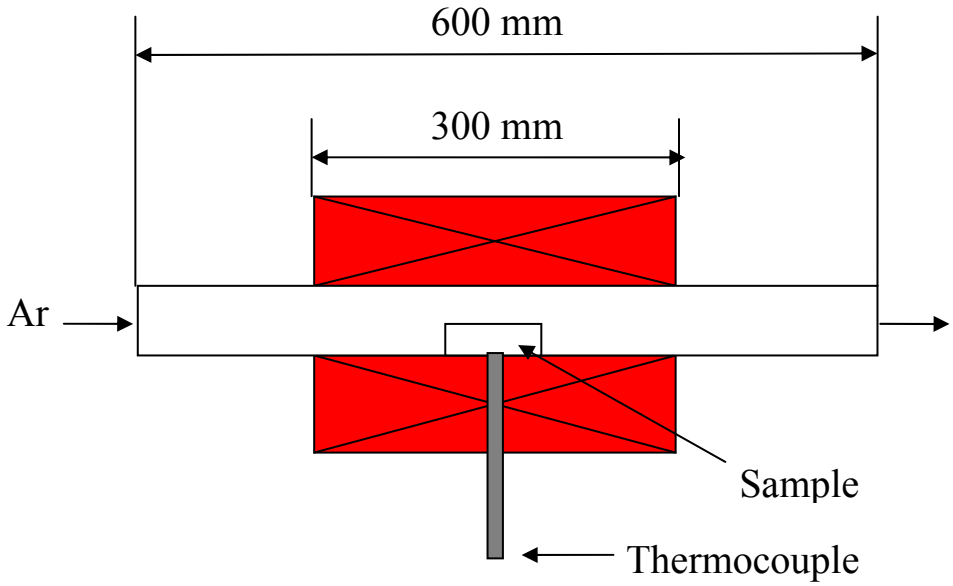


**Figure 2–2 Skeleton diagram of furnace**

**(a)**

**(b)**

**Figure 2–3 Char sample before (a) and after (b) activation**

In each experiment the activation temperature was reached at a 10 $^{o}$C/min heating rate and then maintained for 2–3 h and the impregnation ratio of activating agent/char

was 1–3. Different activation temperatures within the 500–900 $^{o}$C range were also investigated. The activated samples were cooled down under Ar flow (**Figure 2–3** shows the char sample before and after activation), and washed with hydrochloric acid (HCl) and distilled water to remove residual chemical until neutral pH. After being settled down overnight, the washed samples were dried at 20 $^{o}$C in vacuum for 2 h, and then pulverized to pass through a 150 mesh sieve. In this study, the parameters of carbonization temperature (CT), activation temperature (AT), impregnation ratio (IR), holding time (HT) and the kinds of activating agents were examined.

**Table 2–2 Preparation conditions of ACs from black liquor**

| Sample | Carbonization temperature ($^{o}$C) | Activation | | |
|---|---|---|---|---|
| | | Activating agent, Holding time | Activating agent /Char (*w/w* %) | Temperature ($^{o}$C) |
| CT500 | 500 | KOH, 2 h | 2/1 | 800 |
| CT600 | 600 | KOH, 2 h | 2/1 | 800 |
| CT700 | 700 | KOH, 2 h | 2/1 | 800 |
| CT800 | 800 | KOH, 2 h | 2/1 | 800 |
| CT900 | 900 | KOH, 2 h | 2/1 | 800 |
| AT500 | 600 | KOH, 2 h | 2/1 | 500 |
| AT600 | 600 | KOH, 2 h | 2/1 | 600 |
| AT700 | 600 | KOH, 2 h | 2/1 | 700 |
| AT800 | 600 | KOH, 2 h | 2/1 | 800 |
| AT900 | 600 | KOH, 2 h | 2/1 | 900 |
| IR1 | 600 | KOH, 2 h | 1/1 | 900 |

| | | | | |
|---|---|---|---|---|
| IR1.5 | 600 | KOH, 2 h | 3/2 | 900 |
| IR2 | 600 | KOH, 2 h | 2/1 | 900 |
| IR2.5 | 600 | KOH, 2 h | 5/2 | 900 |
| IR3 | 600 | KOH, 2 h | 3/1 | 900 |
| HT0.5 | 600 | KOH, 0.5 h | 2/1 | 600 |
| HT1 | 600 | KOH, 1 h | 2/1 | 600 |
| HT1.5 | 600 | KOH, 2.5 h | 2/1 | 600 |
| HT2 | 600 | KOH, 2 h | 2/1 | 600 |
| HT2.5 | 600 | KOH, 2.5 h | 2/1 | 600 |
| HT3 | 600 | KOH, 3 h | 2/1 | 600 |
| N500 | 600 | NaOH, 2 h | 2/1 | 500 |
| N600 | 600 | NaOH, 2 h | 2/1 | 600 |
| N700 | 600 | NaOH, 2 h | 2/1 | 700 |
| N800 | 600 | NaOH, 2 h | 2/1 | 800 |
| N900 | 600 | NaOH, 2 h | 2/1 | 900 |
| K500 | 600 | $K_2CO_3$, 2 h | 2/1 | 500 |
| K600 | 600 | $K_2CO_3$, 2 h | 2/1 | 600 |
| K700 | 600 | $K_2CO_3$, 2 h | 2/1 | 700 |
| K800 | 600 | $K_2CO_3$, 2 h | 2/1 | 800 |
| K900 | 600 | $K_2CO_3$, 2 h | 2/1 | 900 |
| 500char | 500 | – | – | – |
| 600char | 600 | – | – | – |
| 700char | 700 | – | – | – |
| 800char | 800 | – | – | – |
| 900char | 900 | – | – | – |

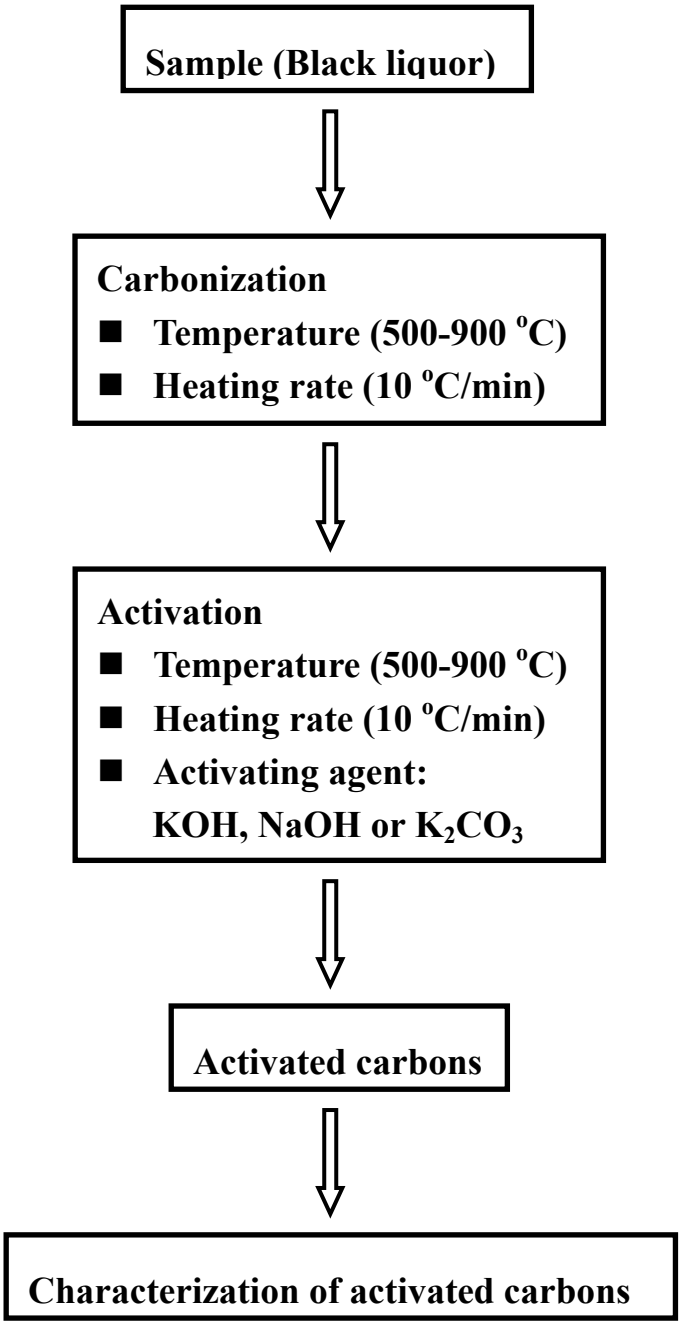


**Figure 2–4 Process flow diagram of experiment**

It is known that washing with acid removes the alkali and alkaline earth metals, and washing with water removes the basic and water-soluble components in the carbon[13]. Thus, the final carbon products obtained by washing will yield well-developed porosity in the carbon structure. This point also was confirmed in Tsai's study[14]. The results

clearly show that the approximate 50% of porosity in the carbon samples should be occupied by potassium salts in the structure. Small surface areas of the unwashed carbons are because of potassium salts left in the carbon products, blocking pore entrances to the nitrogen molecules based on the analysis of adsorption and desorption isotherms of nitrogen for determining BET surface area. Therefore, in this study, the ACs were washed by HCl, and then by water. The preparation conditions of ACs are displayed in **Table 2–2**, and the process flow diagram of experiment is given in **Figure 2–4**.

### 2.2.5 Characterization of ACs and Chars

The adsorption isotherm of $N_2$ was measured on the AC at 77 K by a constant volume adsorption apparatus (BELSORP-max, Japan), and the specific surface area was determined by multi-point BET method. The micropore and mesopore distributions were determined by MP method and DH method, respectively.

BET method is based on the multi-layer molecular adsorption model proposed by Stephen Brunauer, Paul Hugh Emmett and Edward Teller, in which single layer adsorption volume, $V_m$ is correlated with multi-layer adsorption volume, V. This is the famous BET equation. Since BET equation is based on multi-layer adsorption theory, which makes it more accurate to describe real adsorption process, measurement by BET method ensures better accuracy. Through measurement of 3–5 groups of multi-layer adsorption volume by sample at different partial nitrogen pressure, an adsorption isotherm can be plotted with $P/V(P_0-P)$ on the *y*-axis and $P/P_0$ on the *x*-axis according to experimental results. Fit this curve to get a straight line, and then slope, and intercept

can be obtained. Surface area of sample under testing can be calculated from known $V_m$. Based on theory and practice, BET equation fit well with real adsorption process when $P/P_0$ is in the range of 0.35–0.05. Curve linearity is nice too in this range, so this range is preferred for practical measurement.

BET equation[15] is:

$$\frac{P}{V(P_0 - P)} = \frac{1}{Vm \cdot C} + \frac{C-1}{Vm \cdot C} \times (\frac{P}{P_0})$$

## 2.3 Results and Discussion

### 2.3.1 TG Analysis

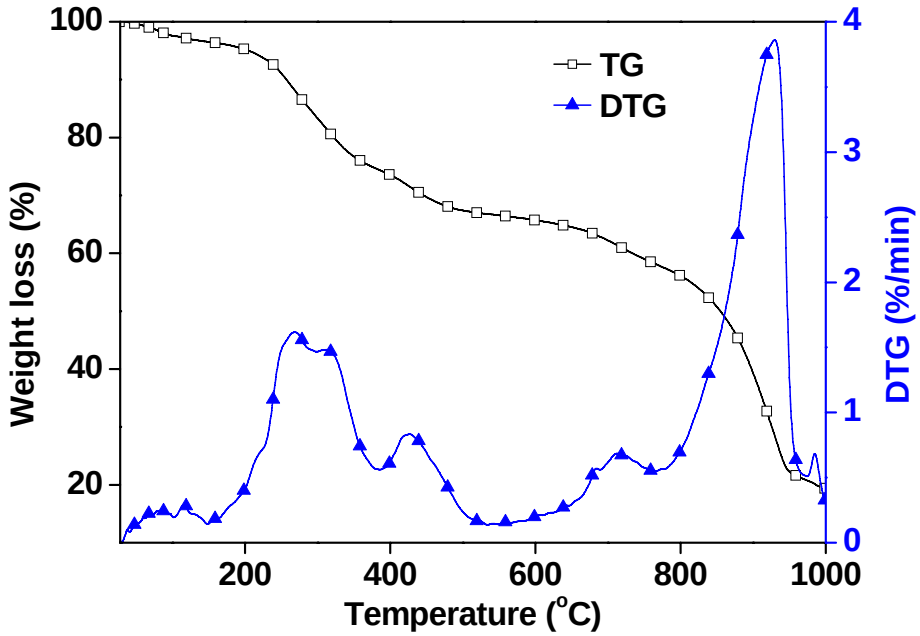


**Figure 2–5 The TG/DTG plots of black liquor**

TG analysis of black liquor revealed that two major thermal decompositions occurred around 250–500 °C and 650–950 °C as shown in **Figure 2–5**. Generally, black

liquor consists of lignin, hemicellulose, cellulose and extracts. From the derivative thermogravimetry (DTG) curve, initial weight loss corresponds to moisture removal, followed by a second degradation event around 250–500 $^{o}$C and a third one around 650–950 $^{o}$C, where the evolution of light volatile compounds occurs from the degradation of cellulose and hemicelluloses. Thermal degradation of these individual components may be superimposed to simulate the overall degradation of black liquor.

### 2.3.2 Char Yields

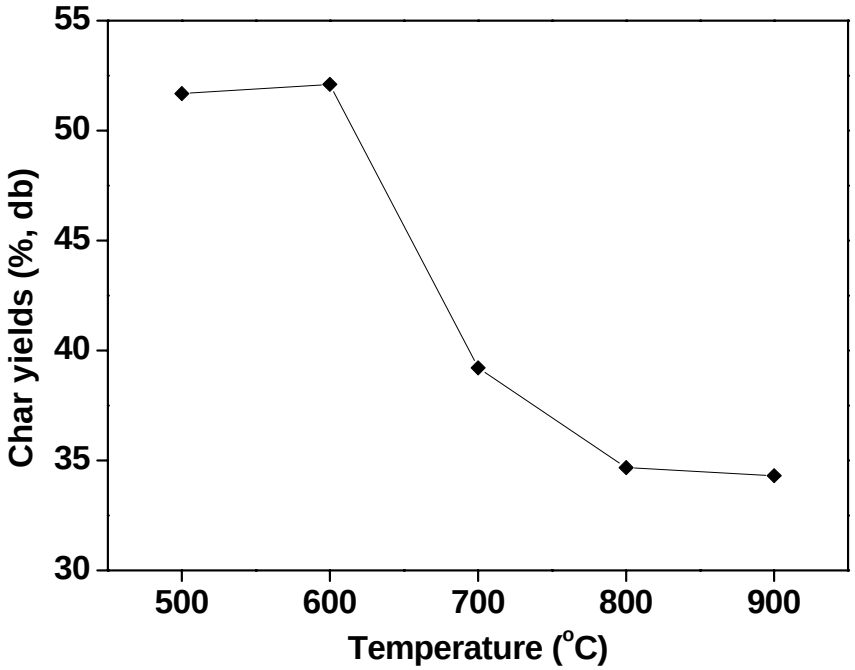


**Figure 2–6 Char yields at different temperatures**

Carbonization temperature plays an important role on the carbonization process. As shown in **Figure 2–6**, the char yield decreases continuously as the raising carbonization temperature. At a lower carbonization temperature (500–600 $^{o}$C), some of the more stable components in small particles may not be readily decomposed, while at higher

temperatures (700–900 $^{o}$C), most of these constituents can be thermally devolatilized, leaving a comparable amount of char.

According to the TG result displayed in **Figure 2–5**, initial weight loss corresponds to moisture removal, followed by a second degradation event around 250–500 $^{o}$C and a major one from 650 to 950 $^{o}$C, in which the evolution of light volatile compounds occurs from the degradation of lignin. It illustrates that the alkali compounds existing in black liquor modify the carbonization behavior of lignin as a chemical reagent in two temperature ranges. Therefore, the char yield decreases rapidly from 700 $^{o}$C, reaching the maximum value at 600 $^{o}$C (52%, db). However, the char yield doesn't decrease rapidly from 800 $^{o}$C to 900 $^{o}$C, according to the major degradation at this temperature range in the DTG plot. This can be explained by carbon deposition during the carbonization process in muffle. These findings are consistent with the general concept that increasing the carbonization temperature decreases the amount of the unstable volatiles on the carbon samples.

**Table 2–3 Characteristic results of char samples**

| Char sample | BET surface area ($m^2$ $g^{-1}$) | Pore volume ($cm^3$ $g^{-1}$) | Pore size (nm) |
|---|---|---|---|
| 500char | 136 | 0.10 | 3.06 |
| 600char | 358 | 0.18 | 2.07 |
| 700char | 478 | 0.26 | 2.20 |
| 800char | 460 | 0.24 | 2.13 |
| 900char | 597 | 0.28 | 1.89 |

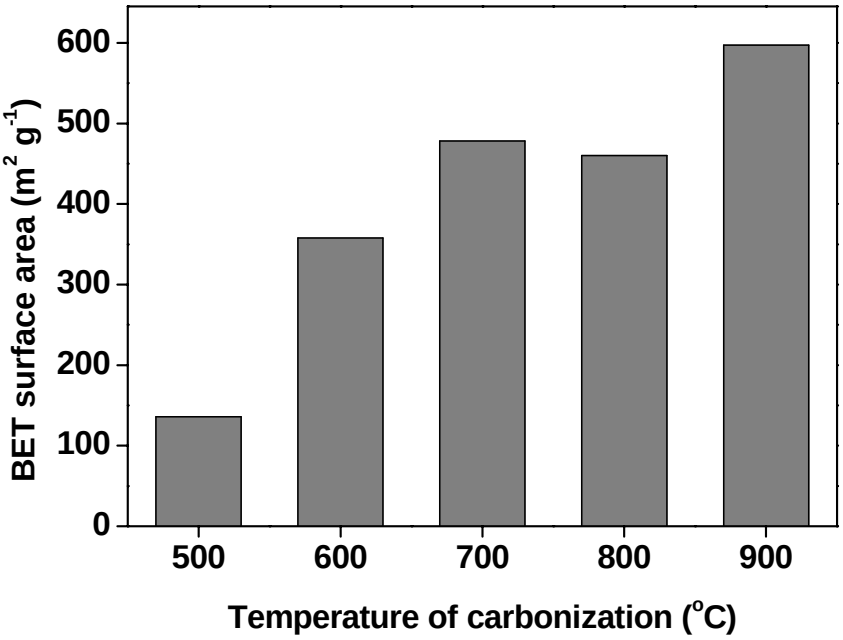


**Figure 2–7 Effect of carbonization temperature on BET surface area of chars**

According to the characteristic results of char samples given in **Table 2–3**, the BET surface area and pore volume roughly increase with the increase of carbonization temperature (shown in **Figure 2–7**). However, pore size decreases following the increasing of carbonization temperature. Hence, 900char shows the highest BET surface area (597 $m^2$ $g^{-1}$) and pore volume (0.28 $cm^3$ $g^{-1}$), along with the smallest pore size (1.8914 nm), which indicates that micropore contributes to the specific surface area.

## 2.3.3 Influence of Carbonization Temperature

It has been indicated that the carbonization process has a great effect on the final product, and careful selection of carbonization parameters is important in order to prepare the required quality of ACs.[16] The purpose of carbonization process is to enrich the carbon content and to create an initial porosity in the char. There are several critical parameters in the preparation of AC that would affect its structure, one of which is

carbonization temperature. It has been shown that high carbonization temperature would result in a great amount of volatiles being released from the raw material and eventually influences the product yield and porosity.[17]

To examine the influence of carbonization temperature on pore structure of ACs, the ACs (named with CT500–900 respectively) were obtained by activating chars with KOH at 800 $^{o}$C for 2 h at the different carbonization temperatures in this section, **Figure 2–8** compares the nitrogen adsorption isotherms of the ACs, and all the samples present type I isotherms, indicating its microporous features.[12] The enhanced volume of the ACs means the increase of pore volume. And the characteristic results of ACs are given in **Table 2–4**.

The surface area and pore size distribution of ACs prepared at different carbonization temperatures (500–900 $^{o}$C) are shown in **Figures 2–9** and **2–10**, respectively. The chars prepared at the carbonization temperature without activation have surface area of 135–600 $m^2$ $g^{-1}$.

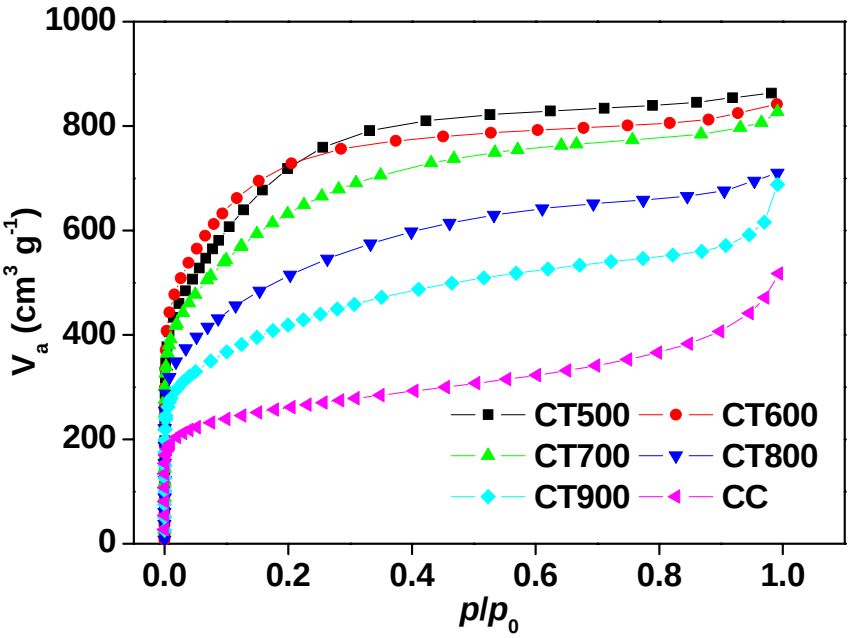


**Figure 2–8 Nitrogen adsorption isotherms of ACs with different carbonization temperatures**

**Table 2–4 Characteristic results of ACs**

| ACs | BET surface area ($m^2\ g^{-1}$) | Pore volume ($cm^3\ g^{-1}$) | Pore size (nm) |
|---|---|---|---|
| BL500 | 2694 | 1.32 | 1.97 |
| BL600 | 2723 | 1.28 | 1.87 |
| BL700 | 2298 | 1.28 | 2.22 |
| BL800 | 1868 | 1.04 | 2.24 |
| BL900 | 1495 | 1.06 | 2.82 |
| CC | 944 | 0.79 | 3.34 |

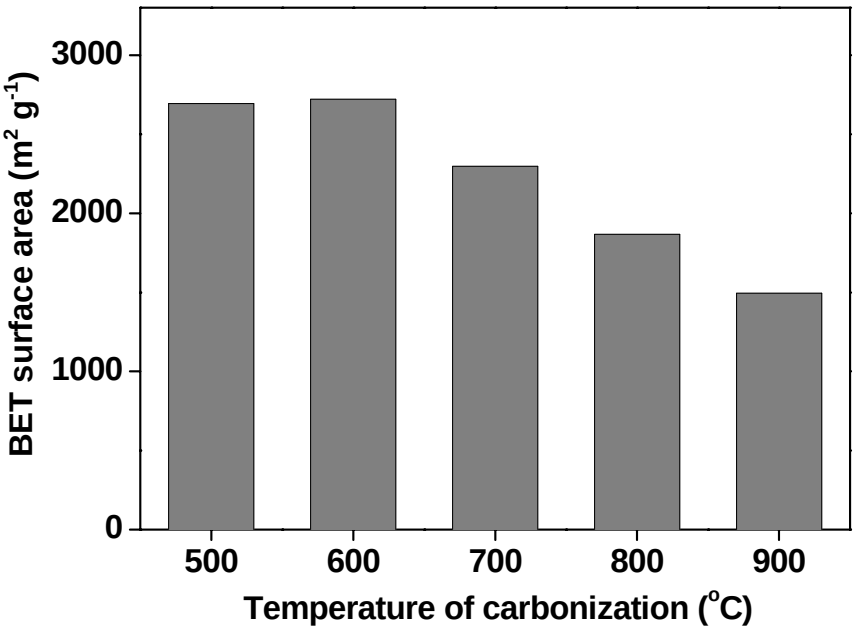


**Figure 2–9 Effect of carbonization temperature on BET surface area**

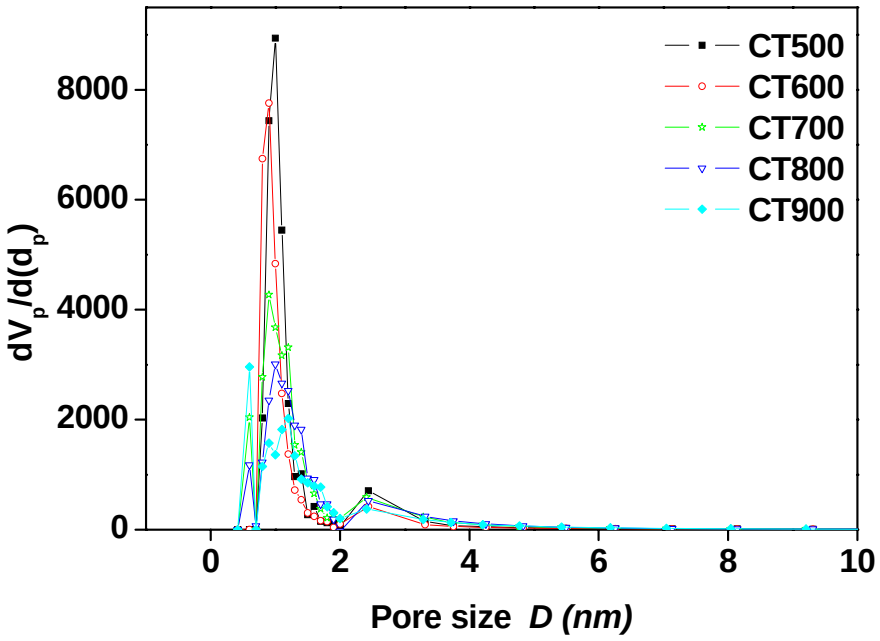


**Figure 2–10 Effect of carbonization temperature on pore size distribution**

It was observed that the surface areas of these ACs are much larger than that of the char, which indicates that KOH works effectively as an activating reagent below 500 $^{o}$C. The surface areas increase between the temperatures of 500 and 600 $^{o}$C, and a maximum surface area of more than 2500 $m^2$ $g^{-1}$ was observed at 600 $^{o}$C. This illustrates that the pores enlarge up to this temperature. Above 600 $^{o}$C, the excess enlargement induces pore combination, resulting in an increase in mesopores, and a decrease of micropore volume and surface area. Hence, the specific surface area and pore volume decreases with the increase of carbonization temperature. From comparison with **Table 2–4**, the ACs prepared from black liquor have surface areas much larger than the commercial AC (labeled CC) prepared from char coal.

### 2.3.4 Influence of Activating Temperature

The activation temperature is considered to be an important parameter that affects

the characteristics of the ACs produced.[18–19] According to the above result, 600 °C char was a potential char for activation in the interest of obtaining porous carbon materials. Consequently, the influence of activation temperatures was examined, and the result is exhibited in **Table 2–5**. **Figure 2–11** compares the nitrogen adsorption isotherms of the ACs (named with AT500-900 respectively), and all the samples also present type I isotherms, indicating its microporous features.

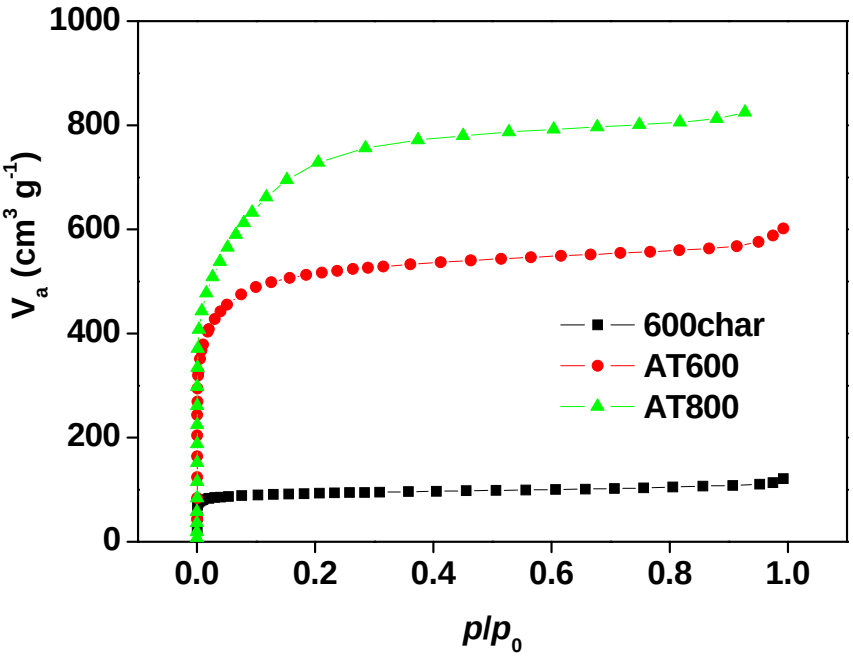


**Figure 2–11 Nitrogen adsorption isotherms of ACs with different activation temperatures**

The BET surface area values corresponding to the ACs obtained at different activation temperatures (500–900 °C) are plotted in **Figure 2–12**. It can be observed that this series of samples covers a wide range of surface areas (from 1900 up to more than 3000 m$^2$ g$^{-1}$), and the BET surface area of the char obtained in 600 °C is only 358 m$^2$ g$^{-1}$. Increasing the temperature from 500 to 900 °C progressively increases both the BET surface and pore volume, reaching 3089 m$^2$ g$^{-1}$ at 900 °C, much larger than usual

commercial ACs, including the ACs prepared from lignin.

**Table 2–5 Characteristic results of ACs**

| ACs | BET surface area ($m^2$ $g^{-1}$) | Pore volume ($cm^3$ $g^{-1}$) | Pore size (nm) |
|---|---|---|---|
| AT500 | 1935 | 0.85 | 1.76 |
| AT600 | 1910 | 0.93 | 1.94 |
| AT700 | 2613 | 1.29 | 1.97 |
| AT800 | 2723 | 1.28 | 1.87 |
| AT900 | 3089 | 1.76 | 2.28 |
| CC | 944 | 0.79 | 3.34 |

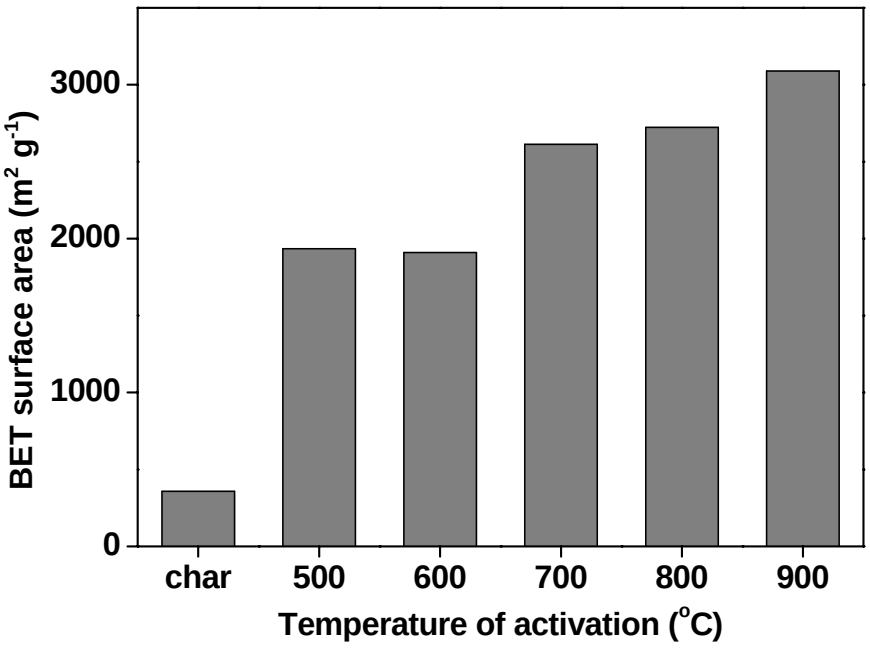


**Figure 2–12** BET surface area of ACs at different activation temperatures.

Because the activation reaction with KOH is an endothermic reaction, so the

enhancement of temperature is propitious to the process of activation reaction and improves the activation effects.[6] Much work has been carried out in the area of chemical activation using KOH. Marsh et al.[20] studied the effect of KOH on different cokes and stated the effect of KOH on different cokes and stated that the presence of oxygen in the alkali resulted in the removal of cross-linking and stabilizing of carbon atoms in the crystallites. Potassium metal liberated at the reaction temperatures may intercalate and force apart the separate lamellae of the crystallite. Removal of these potassium salts (by washing) and carbon atoms (by activation reaction) from the internal volume of the carbon creates the micropores in the structure. Otowa et al.[21,22] produced high-surface-area activated carbons from petroleum coke by KOH and studied the activation mechanisms. They found that considerable amounts of $K_2CO_3$ and hydrogen were formed and only a small amount of $CO_2$ was contained in the effluent gas. Also, they concluded that high temperature would cause several atomic layers of carbon being widened and hence, forming large pores. Some possible reactions were proposed:

$$2\,KOH \rightarrow K_2O + H_2O \text{ (dehydration)}$$

$$C + H_2O \rightarrow H_2 + CO \text{ (water-gas reaction)}$$

$$CO + H_2O \rightarrow H_2 + CO_2 \text{ (water-gas shift reaction)}$$

$$K_2O + CO_2 \rightarrow K_2CO_3 \text{ (carbonate formation)}$$

When the activation temperature exceeds 700 $^oC$, a considerable amount of metallic potassium is formed due to the following possible reaction:

$$K_2O + H_2 \rightarrow 2\,K + H_2O \text{ (reduction by hydrogen)}$$

$$K_2O + C \rightarrow 2\,K + CO \text{ (reduction by carbon)}$$

In this study, increasing the temperature from 500 °C to 900 °C increase of the pore development, and creates new pores. The progressive temperature rise increases the C-KOH reaction rate, resulting in increasing carbon burn-off. Concurrently, the continuous evolution of volatiles from the char samples also increases with increasing temperature. The devolatilization process further develops the rudimentary pore structure in the char, whereas the C-KOH reaction enhances the existing pores and creates new ones. These two reactions produce an increasing BET surface area and micropore volume with increasing activation temperature. The micropore volume is developed as activation temperature increases, which was just as reported that higher micropore volumes and wider micropore sizes would be obtained by KOH activation.[23]

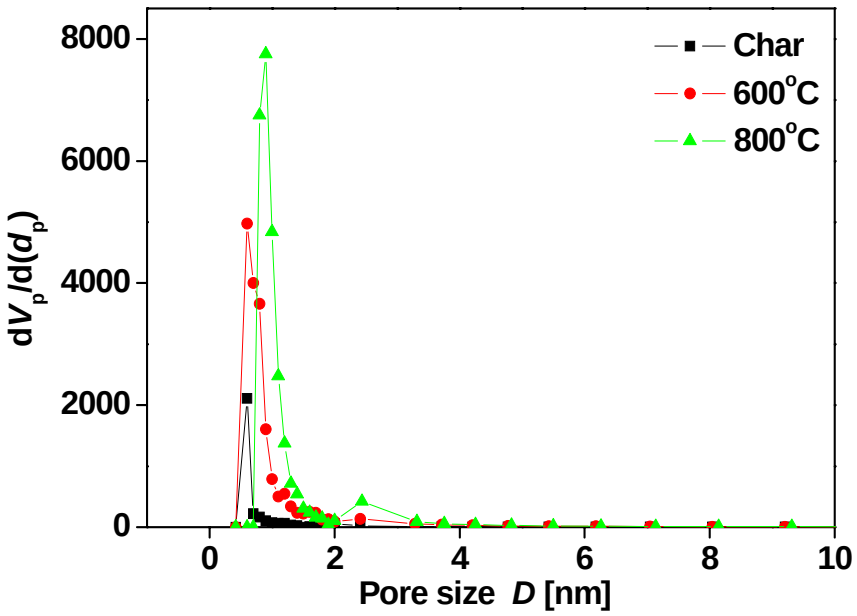


**Figure 2–13 Effect of activation temperature on pore size distribution**

Taking AT600) and AT800 as example, the effect of activation temperature on pore size distribution is given in **Figure 2–13**. It is found that the micropore is well developed with the increase of temperature.

## 2.3.5 Influence of Impregnation Ratio

**Table 2–6 Characteristic results of ACs**

| ACs | BET surface area ($m^2\ g^{-1}$) | Pore volume ($cm^3\ g^{-1}$) | Pore size (nm) |
|---|---|---|---|
| IR1 | 1936 | 1.32 | 2.73 |
| IR1.5 | 2382 | 1.59 | 2.67 |
| IR2 | 3089 | 1.76 | 2.28 |
| IR2.5 | 2865 | 2.22 | 3.09 |
| IR3 | 2448 | 2.04 | 3.34 |
| CC | 944 | 0.79 | 3.34 |

The impregnation ratio of activating agent/char has been found to be one of the important parameter in preparation of AC using chemical activation.[24,25] In order to study the effect of impregnation ratio on the performance of the ACs, here we used carbonization temperature of 600 $^{o}$C and activation temperature of 900 $^{o}$C according to the above result. The pore characteristic of ACs (named with IR1-3 respectively) produced at various impregnation ratios are given in **Table 2–6**, and **Figure 2–14** illustrates the effect of impregnation ratio on BET surface area of the ACs.

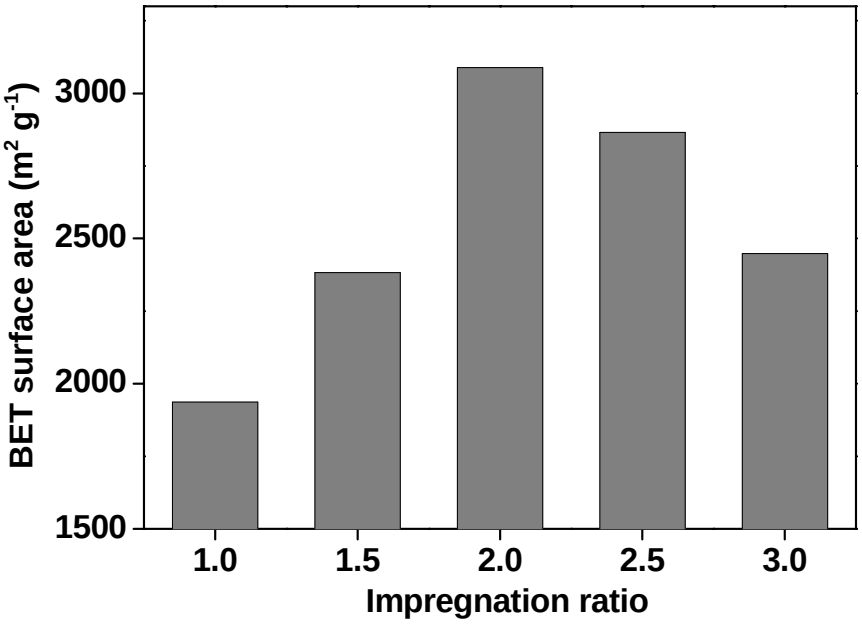


**Figure 2–14 Effect of impregnation ratio on BET surface area**

The result indicates that pore volume is increasing continuously with impregnation ratio, and the BET surface area also increases with impregnation ratio up to 2, and thereafter decreases with increasing ratio above 2. The mechanism of pore evolution with varying ratio is as follows: Upon increasing the ratio from 1 to 2, predominantly micropores but some mesopores or macropores are progressively formed and hence the BET surface area of the ACs continues to increase up to a maximum of 3089 $m^2 g^{-1}$ for a ratio of 2. The presence of hydroxyl group acts as the oxidizer for the C-KOH reaction, resulting in the consumption of carbon and the formation of pores within the internal carbon structures. The continuous devolatilization of the char sample also contributes to the increase in the BET surface area, regardless of the different ratios. When the ratio is increased from 2 to 2.5, the BET surface area decreases slightly, which is attributed to the pore widening effect as the pore walls are "burnt-off" and become thinner. A further

increase of the ratio to 3 results in further reductions in the BET surface area. These reductions are due to an enhanced C-KOH reaction, resulting in the widening of pores through the complete "burning-off" of some walls between neighboring pores and continuous pore wall thinning. In general, since the increase of KOH can accelerate the reaction rate, a great quantity of pores increased correspondingly. However, excessive amount of KOH added can cause further reaction between KOH and carbon of micro-porous structure formed at previous stage. That is to say, addition of excessive amount of KOH may destroy the micro-porous structure and enlarge the volume of pores. Therefore, the amount of KOH played a decisive role for formation of pores.

Based on the above results, the optimum ratio of KOH/char is 2 for maximum BET surface area, and this ratio would be used for the subsequent experiment.

### 2.3.6 Influence of Holding Time

The specific surface area of AC may be influenced by the holding time during activation. In order to find the suitable holding time, the values of BET surface area of ACs (named with HT1-3 respectively) prepared after experiencing different holding time at a carbonization temperature of 600 $^{o}$C, a activation temperature of 600 $^{o}$C and a impregnation ratio of 2 were investigated, and the result is shown in **Table 2–7**. When holding time was 1, 1.5, 2, 2.5 and 3 h, BET surface area of AC was 1556, 1796, 1791, 1910, 1936 and 2140 $m^2$ $g^{-1}$ accordingly.

**Table 2–7 Characteristic results of ACs**

| ACs | BET surface area ($m^2\ g^{-1}$) | Pore volume ($cm^3\ g^{-1}$) | Pore size (nm) |
|---|---|---|---|
| HT0.5 | 1556 | 0.72 | 1.86 |
| HT1 | 1796 | 0.86 | 1.96 |
| HT1.5 | 1791 | 0.83 | 1.86 |
| HT2 | 1910 | 0.93 | 1.94 |
| HT2.5 | 1936 | 0.95 | 1.96 |
| HT3 | 2140 | 1.07 | 2.00 |
| CC | 944 | 0.79 | 3.34 |

**Figure 2–15** shows the surface area characteristics of the ACs. Increasing the holding time from 0.5 to 1 increases the BET surface area and pore volumes. These properties increase with the continuous devolatilization of the char; coupled with pore enhancement and the formation of new pores which are both due to carbon burn off as a result of the C-KOH reaction. However, at a hold time of 1.5 h, the BET surface area and pore volume slightly decrease due to the pore wall thinning effect and the subsequent substantial release of volatiles. When the hold time is increased from 1.5 to 3, the BET surface area and pore volume increase. These increases are due to the formation of new micropores and the conversion of some micropores to meso- and macropores through the C-KOH reaction, besides the continuous release of volatiles from the sample.

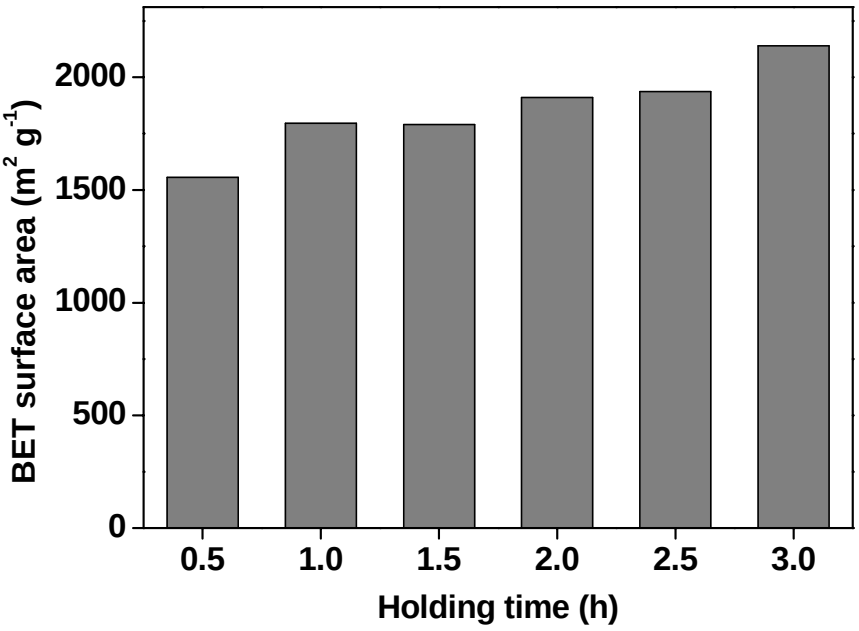


**Figure 2–15 Effect of holding time on BET surface area**

## 2.3.7 Influence of Activating Agents (NaOH)

Among all the chemical activation agents, alkaline hydroxides as KOH or NaOH are reported to be highly interesting from the performance point of view, allowing ACs to be prepared from many kinds of carbonaceous precursors (coals, chars, fibres, etc.) [26–35]. A study[34] suggests that the carbon/MOH (M = Na or K) reaction mechanism is independent of the hydroxide. The hydroxide reduction leads to $H_2$ and Na or K metals, and carbon is oxidized to carbonates (Na or K ) according to the global reaction:

$$6MOH + C \leftrightarrow 2M + 3H_2 + 2M_2CO_3$$

The common feature of all the materials for which NaOH was not an efficient activating agent, was the presence of some organization of the graphene layers. Therefore, the previous statements that carbon activation by NaOH or KOH takes place through the

same reactions are not completely exact.

Raymundo-Piñero et al.[36] have demonstrated that there is a different behavior of NaOH and KOH as activating agents related with the structural organization of the pristine material. NaOH is only effective with disordered materials whereas KOH was found effective with all of them. The differences found between KOH and NaOH during activation are related with an additional intercalation step of metallic K or Na produced during the redox reactions. It is shown that metallic K has the ability to be intercalated in all materials in contrast with Na which can only intercalate in the very disorganised ones.

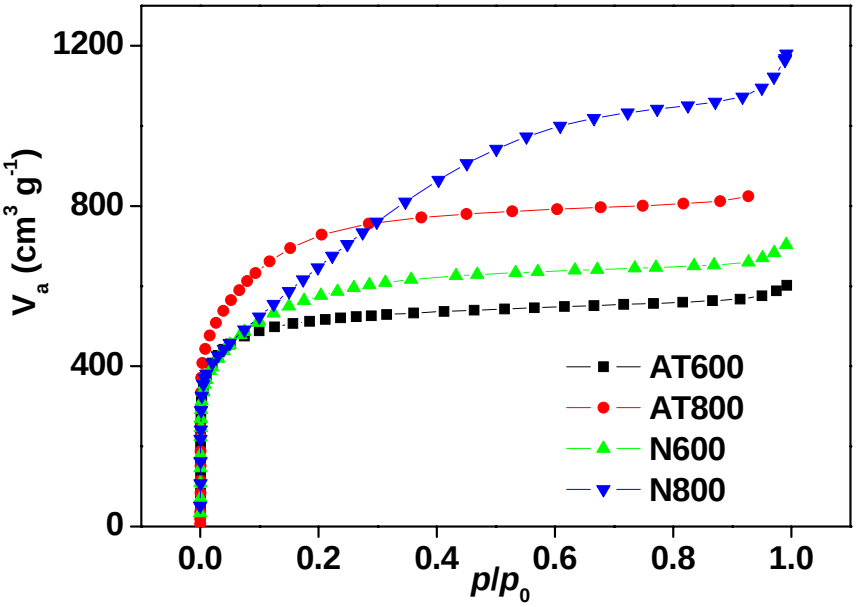


**Figure 2–16 Nitrogen adsorption isotherms of ACs**

In order to study the activation effect of NaOH on performance of the ACs derived from black liquor, here we used carbonization temperature of 600 $^{o}$C and activation temperature of 900 $^{o}$C. **Figure 2–16** compares the nitrogen isotherms of ACs activated by NaOH and KOH with the same carbonization temperature, activation temperature, holding time and impregnation ratio. The pore characteristic of ACs (named with

N500–900 respectively) produced by NaOH activation at various impregnation ratios are given in **Table 2–8**, and **Figure 2–17** compares the activation effect of NaOH and KOH on BET surface area of the ACs at different activation temperatures.

**Table 2–8 Characteristic results of ACs**

| ACs | BET surface area ($m^2\ g^{-1}$) | Pore volume ($cm^3\ g^{-1}$) | Pore size (nm) |
|---|---|---|---|
| N500 | 1775 | 0.86 | 1.95 |
| N600 | 2082 | 1.08 | 2.08 |
| N700 | 2699 | 1.60 | 2.38 |
| N800 | 2448 | 1.81 | 2.95 |
| N900 | 759 | 0.62 | 3.26 |
| CC | 944 | 0.79 | 3.34 |

The results show that the activation effect of NaOH and KOH is different. In KOH activation which was discussed in section 2.3.4, increasing the temperature from 500 $^{o}$C to 900 $^{o}$C progressively increases both the BET surface and pore volume. However, in NaOH activation, the BET surface area increases with the increase of activation temperature until 700 $^{o}$C, and then decreases from 700 to 900 $^{o}$C, especially at 900 $^{o}$C. This decrease in surface area is comparable. As temperature increased, ash formation also increased, resulting in decrease of surface area. Pore widening and pore collapse could also occur and result in decrease of surface area. Researchers have also observed that beyond a certain temperature (depending on raw material, method of activation and other

parameters), the surface area of the ACs decreased.

As mentioned above, because the activation reaction with NaOH is an endothermic reaction, so the enhancement of temperature is propitious to the process of activation reaction and improves the activation effects. However, since the increase of temperature can accelerate the reaction rate, a great quantity of pores increased correspondingly; Above 700 $^{o}$C, the excess enlargement induces combination of pores, resulting in an increase in mesopores for all alkali metal salts, and a decrease of micropore volume, and of surface area.

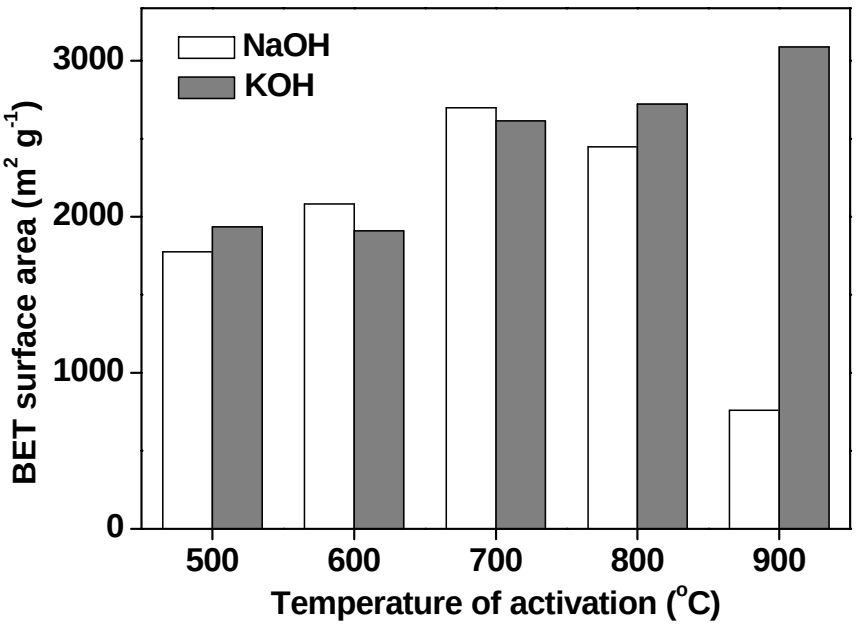


**Figure 2–17 Effect of activation temperature on BET surface area**

## 2.3.8 Influence of Activating Agents ($K_2CO_3$)

$K_2CO_3$ is not a hazardous chemical and not deleterious, so it is also frequently used for activtating agent replacing KOH and NaOH.[37] In order to investigate the activation

effect of $K_2CO_3$ on performance of the ACs derived from black liquor, here we used the same experiment condition used in section **2.3.7**. The pore characteristic of ACs (named with K500–900 respectively) produced by $K_2CO_3$ activation at various impregnation ratios are given in **Table 2–9**, and **Figure 2–18** compares the activation effect of $K_2CO_3$ and KOH on BET surface area of the ACs at different activation temperatures.

**Table 2–9 Characteristic results of ACs**

| ACs | BET surface area ($m^2\ g^{-1}$) | Pore volume ($cm^3\ g^{-1}$) | Pore size (nm) |
|---|---|---|---|
| K500 | 339 | 0.18 | 2.09 |
| K600 | 358 | 0.20 | 2.19 |
| K700 | 790 | 0.37 | 1.87 |
| K800 | 1026 | 0.47 | 1.84 |
| K900 | 1136 | 0.61 | 2.15 |
| CC | 944 | 0.79 | 3.34 |

According to the result, the BET surface area increases with the increase of activation temperature similar to KOH activation, although the values of BET surface area are much lower than that in KOH activation. The surface areas of the ACs prepared by $K_2CO_3$ activation at 500 $^oC$ and 600 $^oC$ are very small, almost the same value as that of the char without activation. It can be presumed that the micro- or mesopore structure was scarcely modified. Thus it was deduced that $K_2CO_3$ activation did not work effectively below 500 $^oC$. This indicates that $K_2CO_3$ is effective above a temperature of

700 $^{o}$C. $K_2CO_3$ was reduced in inert atmosphere by carbon as follows:[38]

$$K_2CO_3 + 2C \rightarrow 2K + 3CO$$

This progressive temperature increased the C–$K_2CO_3$ reaction rate, resulting in increasing carbon "burn-off". Concurrently, the volatiles from the samples continued to evolve with increasing carbonization temperature. The develotilization process further developed the rudimentary pore structure in the char, whereas the C-$K_2CO_3$ reaction enhanced the existing pores and created new porosities.

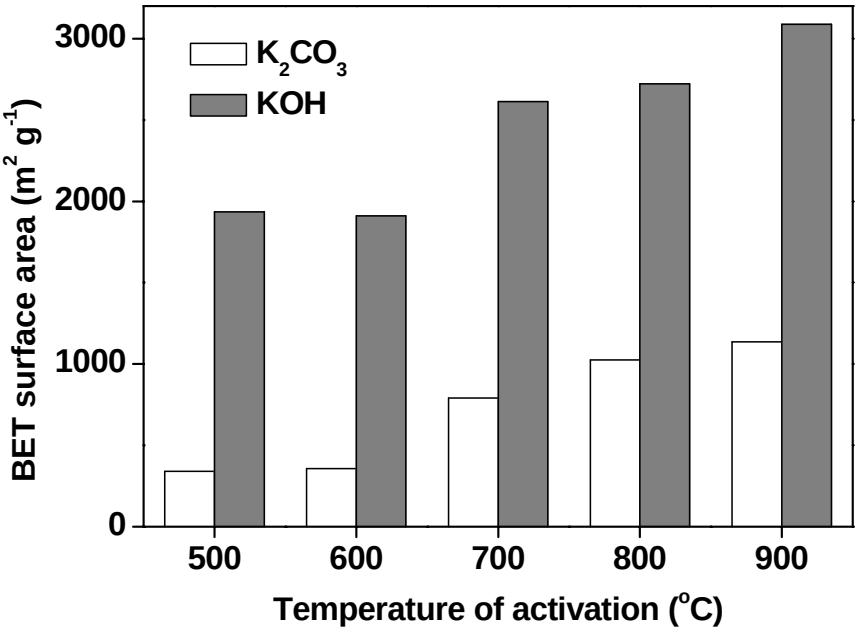


**Figure 2–18 Effect of activation temperature on BET surface area**

## 2.3.9 Influence of the Presence of Na and K

As shown in **Table 2–2**, high content of Na (32.1 mg/g) and K (3.0 mg/g) exist in black liquor, which are effectively used to improve the activation process. In order to

investigate the influence of the presence of Na and K, 600 °C char was washed by HCl and distilled water until neutral pH to remove the residual alkali metal in black liquor. Then, the pore characterization of the AC (named with ACdaf900) prepared from the eluted char was compared with AC900 at the same preparation condition, and the results are given in **Table 2–10**.

**Table 2–10 Characteristic results of ACs**

| ACs | BET surface area ($m^2\ g^{-1}$) | Pore volume ($cm^3\ g^{-1}$) | Pore size (nm) |
|---|---|---|---|
| AC900 | 3089 | 1.76 | 2.28 |
| ACdaf900 | 1245 | 0.66 | 2.11 |
| Char | 358 | 0.18 | 2.07 |

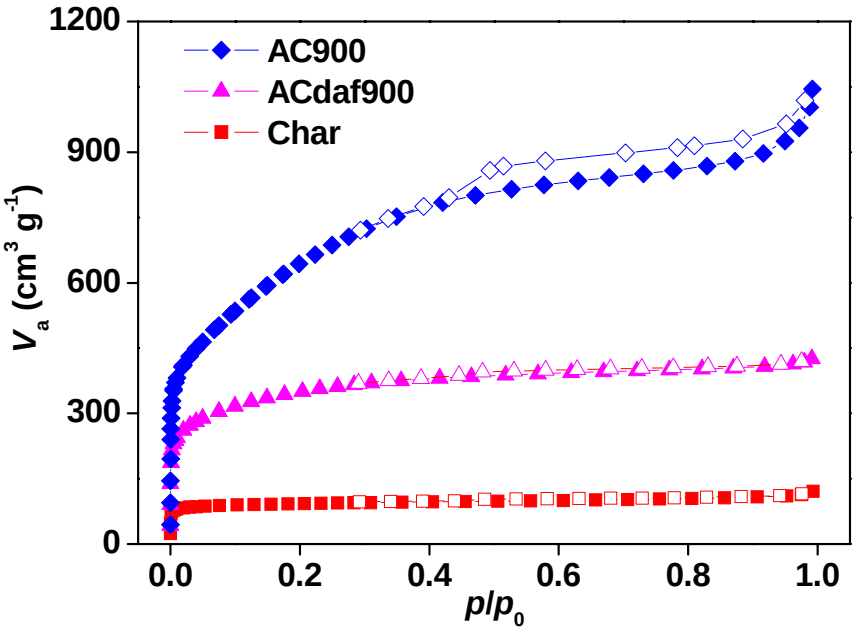


**Figure 2–19 $N_2$ adsorption-desorption isotherms of ACs: Closed symbols, adsorption; open symbols, desorption**

Figure **2–19** and Figure **2–20** give the characteristic of ACs and char. According to

IUPAC classification, the char and ACdaf900 exhibit a steep type I isotherms. Adsorption curve rose sharply at relative pressure of $p/p_0$ less than 0.10, and then approached plateau with increasing relative pressure; the adsorption and desorption branches were parallel over a wide range at higher relative pressure, indicating its microporous characterization. Whereas, AC900 exhibits a combination isotherm of type I and II, indicating the presence of some mesopores in the carbon corpuscular.

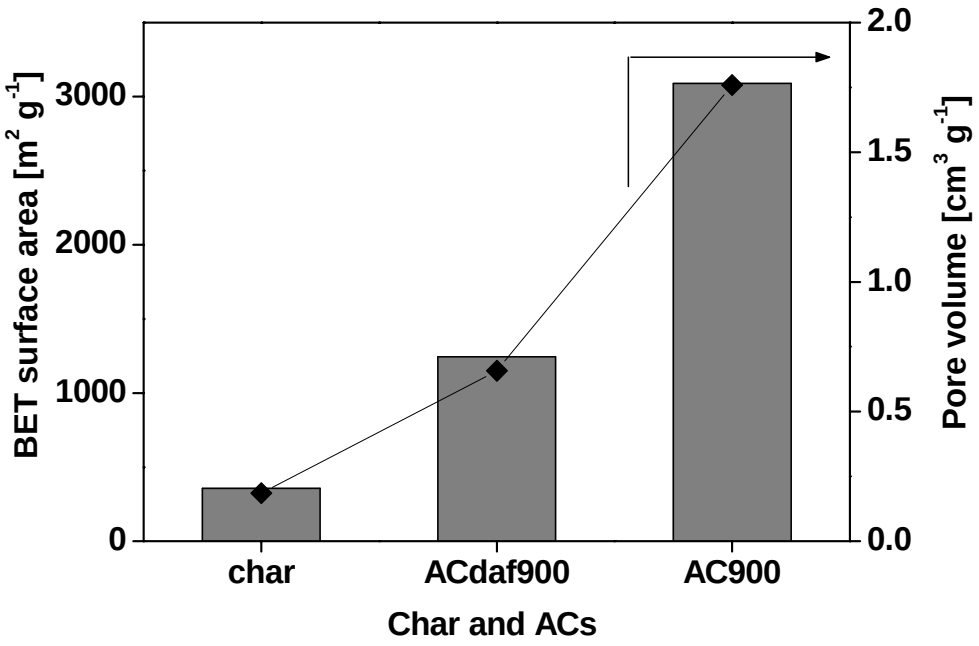


**Figure 2–20 BET surface area and pore volume of char and ACs**

Besides, the result given in **Figure 2–20** explains that ACdaf900 shows much lower BET surface area and pore volume than AC900. It illuminates that the alkali metals that exist in black liquor did react as activating agent in the process of activation, which explains that why the amount of KOH used in this study was extremely economized comparing with previous researches as given in **Table 2–11**.[4, 39–42]

**Table 2–11 Comparison with other researches**

| Raw material | KOH/Char (w/w) | BET surface area ($m^2$ $g^{-1}$) | Reference |
|---|---|---|---|
| Black liquor | 2/1 | 3089 | |
| Cassava peel | 5/2 | 1605 | Sudaryanto et al., 2006 |
| Raw pitch coke | 4/1 | 2320 | Mitani et al., 2004 |
| Olive-seed waste residue | 4/1 | 3049 | Stavropoulos et al., 2005 |
| Edible red sugar cane | 6/1 | 2299 | Tseng et al., 2006 |
| Fir wood | 6/1 | 2794 | Wu et al., 2005 |

## 2.4 Summaries

ACs with large surface area were prepared from chemical activation of black liquor with KOH, NaOH and $K_2CO_3$. Among which, KOH is the most effective activating agent for activation with black liquor. The results show that the porosity of the ACs is highly dependent on the preparation conditions, such as carbonization temperature, activation temperature, holding time and chemical impregnation ratio. Under the experimental conditions studied, the best conditions for preparing ACs with high surface area and pore volume are an carbonization temperature of 600 $^oC$, an activation temperature of 900 $^oC$, and an impregnation ratio of 2 (KOH to char). With these experimental conditions, an AC with a BET surface area of 3089 $m^2$ $g^{-1}$ and a total pore volume of 1.76 $cm^3$ $g^{-1}$ was obtained. Besides, the optimal impregnation ratio of 2 is much lower than those recommended in the literature. Too high impregnation ratio will result in the burn-off of

carbon structures and widening of the micropores. The amount of activating agent used in this study was extremely economized comparing with previous researches. Accordingly, black liquor was demonstrated to be an excellent and low-cost candidate for manufacturing ACs with good pore characteristics.

## 2.5 References


(1) Hu, Z.H.; Srinivasan, M.P. Preparation of high-surface-area activated carbons from coconut shell. *Microporous Mesoporous Mater.* **1999**, *27*(1), 11–18.

(2) Dias, J.M.; Alivim-Ferraz, M.C.M.; Almeida, M.F.; Rovera-Utrolla, J.; Sánchez-Polo, M. Waste materials for activated carbon preparation and its use in aqueous- phase treatment: a review. *J. Environ. Manage.* **2007**, *85*(4), 833–846.

(3) Qian, Q.R.; Machida, M.; Tatsumoto, H. Preparation of activated carbons from cattle-manure compost by zinc chloride activation. *Bioresour. Techenol.* **2007**, *98*(2), 353–360.

(4) Tseng, R.L.; Tseng, S.K. Characterization and use of high surface area activated carbons prepared from cane pith for liquid-phase adsorption. *J. Hazard. Mater.* **2006**, *136*(3), 671–680.

(5) Roh, K.C.; Park, J.B.; Lee, C.T.; Park, C.W. Study on synthesis of low surface area activated carbons using multi-step activation for use in electric double layer capacitor. *J. Ind. Eng. Chem.* **2008**, *14*(2), 247–251.

(6) Zhao, X.Y.; Cao, J.P.; Morishita, K.; Ozaki, J.; Takarada, T. Electric double-layer capacitors from activated carbon derived from black liquor. *Energy Fuels* **2010**, *24*(3),

1889–1893.

(7) Pollard, S.J.T.; Fowler, G.D.; Sollars, C.J.; Perry, R. Low-cost adsorbents for waste and wastewater treatment: A review. *Sci. Total Environ.* **1992**, *116*(1–2), 31–52.

(8) Demirbaş, A. Pyrolysis and steam gasification processes of black liquor. *Energy Convers. Manage.* **2002**, *43*(7), 877–884.

(9) Hayashi, J. Kazehaya, A.; Muroyama, K.; Watkinson, A.P. Preparation of activated carbon from lignin by chemical activation. *Carbon* **2000**, *38*(13), 1873–1878.

(10) Gonzalez-Serrano, E.; Cordero, T.; Rodriguez-Mirasol, J.; Cotoruelo, L.; Rodriguez, J.J. Removal of water pollutants with activated carbons prepared from H3PO4 activation of lignin from kraft black liquor. *Water Res.* **2004**, *38*(13), 3043–3050.

(11) Zaied, M.; Bellakhal, N. Electrocoagulation treatment of black liquor from paper industry. *J. Hazard. Mater.* **2009**, *163*(2–3), 995–1000.

(12) Veksha, A.; Sasaoka, E.; Uddin, M.A. The effects of temperature on the activation of peat char in the presence of high calcium content. *J. Anal. Appl. Pyrolysis* **2008**, *83*(1), 131–136.

(13) Ahmadpour, A.; Do, D.D. The preparation of active carbons from coal by chemical and physical activation. *Carbon* **1996**, *34*(4), 471–479.

(14) Tsai, W.T.; Chang, C.Y.; Wang, S.Y.; Chang, C.F.; Chen, S.F.; Sun, H.F. Preparation of activated carbons from corn cob catalyzed by potassium salts and subsequent gasification with $CO_2$. *Bioresour. Techenol.* **2001**, *78*(2), 203–208.

(15) Brunauer, S.; Emmett, P.H.; Teller, E. Adsorption of gases in multimolecular layers. *J. Am. Chem. Soc.* **1938**, *60*(2), 309–319.

(16) Li, W.; Yang K.B.; Peng, J.H.; Zhang, L.B; Guo, S.H.; Xia, H.Y. Effects of carbonization temperatures on characteristics of porosity in coconut shell chars and activated carbons derived from carbonized coconut shell chars. *Ind. Crops Prod.* **2008**, *28*(2), 190–198.

(17) Daud, W.M.A.W.; Ali, W.S.W.; Sulaiman, M.Z. The effects of carbonization temperature on pore development in palm-shell-based activated carbon. *Carbon* **2000**, *38*(14), 1925–1932.

(18) Yang, T.; Lua, A.C. Characteristics of activated carbons prepared from pistachio-nut shells by potassium hydroxide activation. *Microporous Mesoporous Mater.* **2003**, *63*(1–3), 113–124.

(19) Sricharoenchaikul, V.; Pechyen, C.; Aht-ong, D.; Atong, D. Preparation and characterization of activated carbon from the pyrolysis of physic nut (Jatropha curcas L.) waste. *Energy Fuels* **2008**, *22*(1), 31–37.

(20) Marsh, H; Yan, D.S.; O'grady, T.M.; Wennerberg, A. Formation of active carbons from cokes using potassium hydroxide. *Carbon* **1984**, *22*(6), 603–611.

(21) Otowa, T.; Nojima, Y.; Miyazaki, T. Development of KOH activated high surface area carbon and its application to drinking water purification. *Carbon* **1997**, *35*(9), 1315–1319.

(22) Otowa, T.; Tanibata, R.; Itoh, M. Production and adsorption characteristics of MAXSORB: High-surface-area active carbon. *Gas Sep. Purif.* **1993**, *7*(4), 241–245.

(23) Suhas; Carrott, P.J.M.; Ribeiro Carrott, M.M.L. Lignin-from natural adsorbent to activated carbon: a review. *Bioresour. Techenol.* **2007**, *98*(12), 2301–2312.

(24) Li, W.; Zhang, L.B.; Peng, J.H.; Li, N.; Zhu, X.Y. Preparation of high surface area activated carbons from tobacco stems with $K_2CO_3$ activation using microwave radiation. *Ind. Crops Prod.* **2008**, *27*(3), 341–347.

(25) Yorgun, S.; Vural, N.; Demiral, H. Preparation of high-surface area activated carbons from Paulownia wood by $ZnCl_2$ activation. *Microporous Mesoporous Mater.* **2009**, *122*(1–3), 189–194.

(26) Yamashita, Y.; Ouchi, K. Influence of alkali on the carbonization process-I: Carbonization of 3,5-dimethylphenol-formaldehyde resin with NaOH. *Carbon* **1982**, *20*(1), 41–45.

(27) Yamashita, Y.; Ouchi, K. Influence of alkali on the carbonization process-II: Carbonization of various coals and asphalt with NaOH. *Carbon* **1982**, *20*(1), 47–53.

(28) Yamashita, Y.; Ouchi, K. Influence of alkali on the carbonization process-III: Dependence on type of alkali and of alkali earth compounds. *Carbon* **1982**, *20*(1), 55–58.

(29) McKee, D.W. Gasification of graphite in carbon dioxide and water vapor-the catalytic effects of alkali metal salts. *Carbon* **1982**, *20*(1), 59–66.

(30) Hu, Z; Vansant, E.F. Synthesis and characterization of a controlled-micropore- size carbonaceous adsorbent produced from walnut shell. *Micropor. Mater.* **1995**, *3*(6), 603–612.

(31) Oh, G.H.; Park, C.R. Preparation and characteristics of rice-straw-based porous carbons with high adsorption capacity. *Fuel* **2002**, *81*(3), 327–336.

(32) Guo, J.; Lua, A.C. Textural and chemical characterizations of adsorbent prepared

from palm shell by potassium hydroxide impregnation at different stages. *J. Colloid Interf. Sci.* **2002**, *254*(2), 227–233.

(33) Diaz-Teran, J.; Nevskaia, D. M.; Fierro, J. L. G.; Lopez-Peinado, A. J.; Jerez, A. Study of chemical activation process of a lignocellulosic material with KOH by XPS and XRD. *Micropor. Mesopor. Mater.* **2003**, *60*(1–3), 173–181.

(34) Lillo-Ródenas, M.A.; Juan-Juan, J.; Cazorla-Amorós, D.; Linares-Solano, A. About reactions occurring during chemical activation with hydroxides. *Carbon* **2004**, *42*(7), 1371–1375.

(35) Xue, R.; Shen, Z. Formation of graphite-potassium intercalation compounds during activation of MCMB with KOH. *Carbon* **2003**, *41*(9), 1862–1864.

(36) Raymundo-Piñero, E.; AzaÏs, P.; Cacciaguerra, T.; Cazorla-Amorós, D.; Linares-Solano, A.; Béguin, F. KOH and NaOH activation mechanisms of multiwalled carbon nanotubes with different structural organisation. *Carbon* **2005**, *43*(4), 786–795.

(37) Adinata, D.; Daud, W.M.A.W.; Aroua, M.K. Preparation and characterization of activated carbon from palm shell by chemical activation with $K_2CO_3$. *Bioresour. Techenol.* **2007**, *98*(1), 145–149.

(38) McKee, D.W. Mechanisms of the alkali metal catalysed gasification of carbon. *Fuel* **1983**, *62*(2), 170–175.

(39) Mitani, S.; Lee, S.I.; Yoon, S.H.; Korai, Y.; Mochida, I. Activation of raw pitch coke with alkali hydroxide to prepare high performance carbon for electric double layer capacitor. *J. Power Sources* **2004**, *133*(2), 298–301.

(40) Sudaryanto, Y.; Hartono, S.B.; Irawaty, W.; Hindarso, H.; Ismadji, S. High surface area activated carbon prepared from cassava peel by chemical activation. *Bioresour. Techenol.* **2006**, *97*(5), 734–739.

(41) Stavropoulos, G.G.; Zabaniotou, A.A. Production and characterization of activated carbons from olive-seed waste residue. *Microporous Mesoporous Mater.* **2005**, *82*(1–2), 79–85.

(42) Wu, F.C.; Tseng, R.L.; Juang, R.S. Preparation of highly microporous carbons from fir wood by KOH activation for adsorption of dyes and phenols from water. *Step. Purif. Technol.* **2005**, *47*(1–2), 10–19.

# Chapter 3 EDLC from AC Derived from Black Liquor

## 3.1 Introduction

EDLCs are very attractive as a potential energy storage system because of their high power density, quick charge-discharge rate, free maintenance, long life operation, and environmentally friendly energy technology.[1–2] For the application, ACs are recognized as an essential component because of their large surface area, highly porous structure, and good adsorption property. Therefore, many researches on ACs with excellent capacitive performance in aqueous[3–6] and nonaqueous[7–8] electrolytes were reported.

Black liquor is one of the main by-product of pulp paper industry, which is considered as pollutant because it contains about 50% of lignin. At present, more than ten kinds of technologies have been utilized extensively, including alkali recovery, acidic separation, biochemistry, membrane treatment, flocculating settling oxygenation, etc.[9] Although these methods of treatment seem effective for the liquid waste processing of paper industry, they present the disadvantage of being expensive because of their operating cost and/or the relatively high cost for the chemical reagents used.[10] Depending on the paper process, high content of compounds of Na, K, etc. exist in black liquor, which are effectively used to improve the activation process. The addition of potassium and sodium compounds is common practice in the production of ACs. Besides the enhancement of reactivity, they are known to promote the development of microporosity

and high surface area.[11] Therefore, using black liquor as a porous carbon precursor may provide an effective approach to carry out the value-added utilization of black liquor. Comparing with the above dispose methods such as alkali recovery, it is more economical and effective, but to some extent, no literature about preparation of EDLC from porous carbon derived from black liquor has been reported in detail.

In this chapter, I tried to prepare EDLC from ACs derived from black liquor. The capacitance of the ACs was evaluated with galvanostatic charge/discharge in 0.5 M TEABF4/PC, and the effects of preparation parameters on the capacitance of the resulting products were investigated.

## 3.2 Experimental

A mixture of 87 wt.% of AC, 10 wt.% of acetylene black and 3 wt.% of PTFE binder was pressed into pellets (13 mm in diameter) as the electrodes. Then the electrodes were dried under vacuum at 200 $^{o}$C for 2 h. Button-type capacitor was assembled with two AC electrodes using 0.5 M TEABF4/PC as the electrolyte as shown in **Figure 3–1**. The capacitors were galvanostatically cycled between 0 and 2.5 V on a Land cell tester. The gravimetric capacitance ($C_g$) of a single electrode was determined with the formula:

$$C_g = I dT / 2 dV$$

where I is the discharge current, $dT$ is the discharge time variation, $dV$ is the voltage variation in discharge.

The volumetric capacitance ($C_v$) was determined with the formula:

$$C_v = C_g \times \rho \times 0.87$$

where $\rho$ is the average density of electrodes. The value of capacitance is calculated with the discharge current density of 10 mA $g^{-1}$ between 1 and 2 V. The preparation conditions all ACs in this study were exhibited in **Table 2–1** in chapter 2.

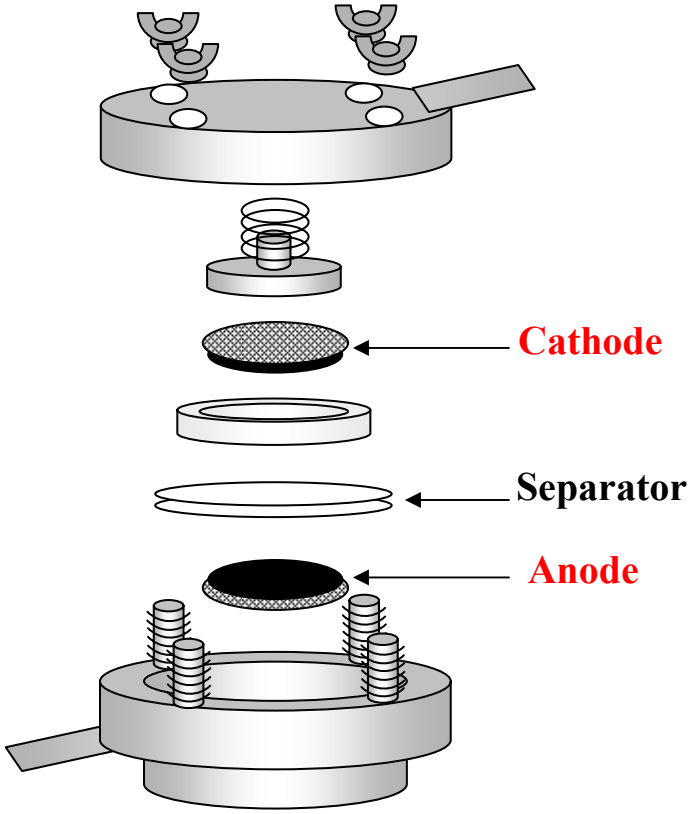


**Figure 3–1 Button-type capacitor**

## 3.3 Results and Discussion

### 3.3.1 Influence of Carbonization Temperature

The ACs were obtained by activating chars with KOH at 800 $^{o}$C for 2 h (named with CT500–900 respectively), and the effect of carbonization temperatures on the BET surface area is discussed in last chapter. **Table 3–1** shows the values of BET surface area and capacitance of ACs, and the charge-discharge curves with a charge current density of 40 mA $g^{-1}$ and a discharge density of 10 mA $g^{-1}$ are given in **Figure 3–2**.

**Table 3–1 BET surface area and capacitance of ACs**

| ACs | BET surface area ($m^2$ $g^{-1}$) | Capacitance (F $g^{-1}$) | Capacitance (F $cm^{-3}$) |
|---|---|---|---|
| CT500 | 2694 | 35.0 | 9.9 |
| CT600 | 2723 | 40.8 | 12.1 |
| CT700 | 2298 | 34.6 | 9.9 |
| CT800 | 1868 | 30.0 | 9.1 |
| CT900 | 1495 | 21.0 | 8.6 |
| CC | 944 | 16.0 | 8.1 |

The results of some previous investigations[12–16] showed that there is a direct relationship between BET surface area and the capacitance of porous carbons. Theoretically, the higher the specific surface area of an AC, the higher the specific

capacitance should be expected. Practically, the situation is more complicated. Significant deviation from this simple law has been frequently observed.[14–18]

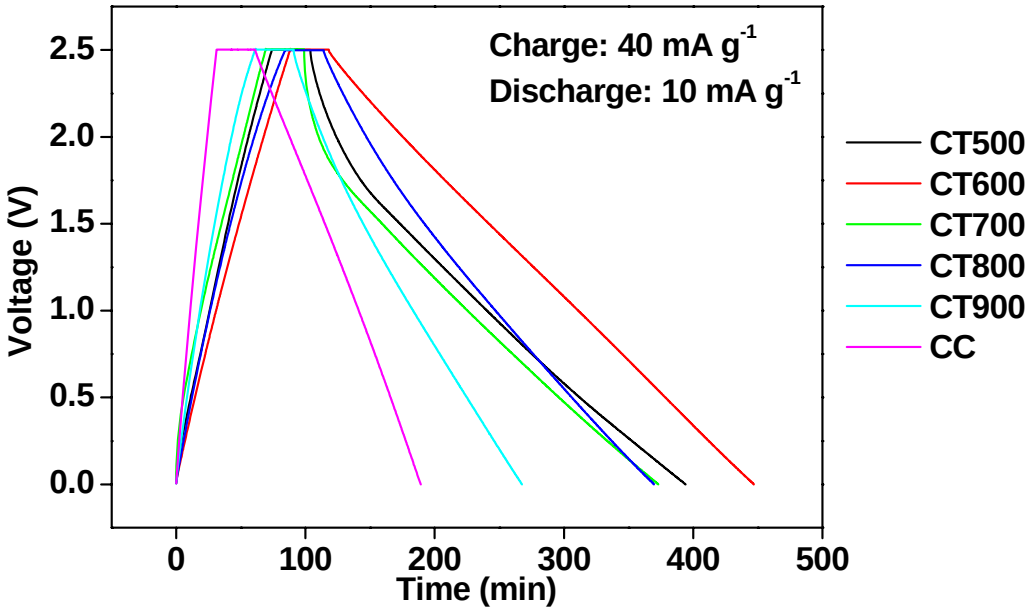


**Figure 3–2 Charge-discharge curves of the ACs-based EDLC**

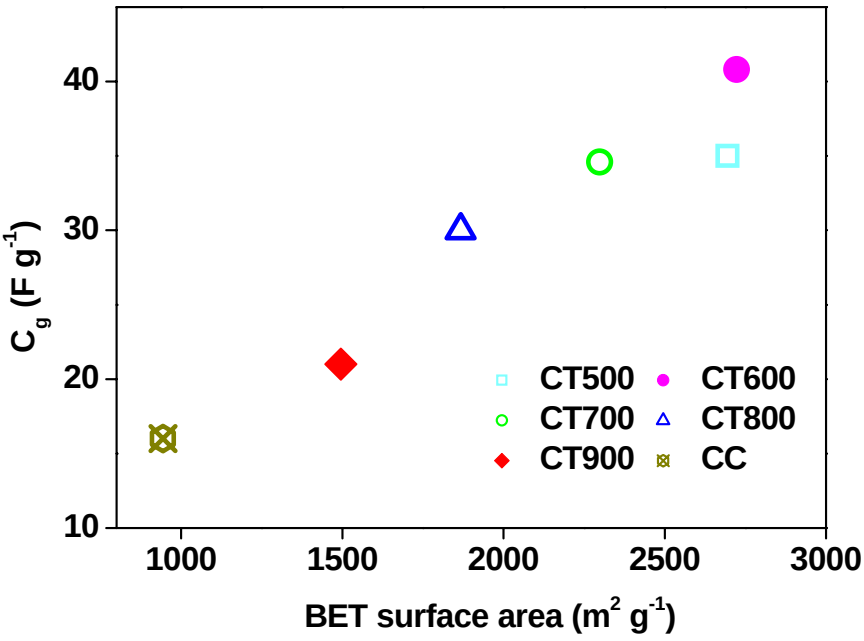


**Figure 3–3 Effect of carbonization temperatures on $C_g$ of ACs**

The effect of carbonization temperature on the specific capacitance of ACs at a current density of 10 mA $g^{-1}$ is illustrated in **Figure 3–3**. It shows that a general trend between capacitance and BET surface area, although it is not a perfect linear relationship. The specific capacitance of CC is only 16.0 F $g^{-1}$. From 600 to 900 $^{o}$C, as the carbonization temperature increases, the capacitance of ACs decreases continuously. CT600 with the highest BET surface area has the highest specific capacitance of 40.8 F $g^{-1}$, twice larger than that of CT900, 2.5 times larger than that of CC. This means that the enhanced capacitance can be mainly attributed to the enhancement of surface area.

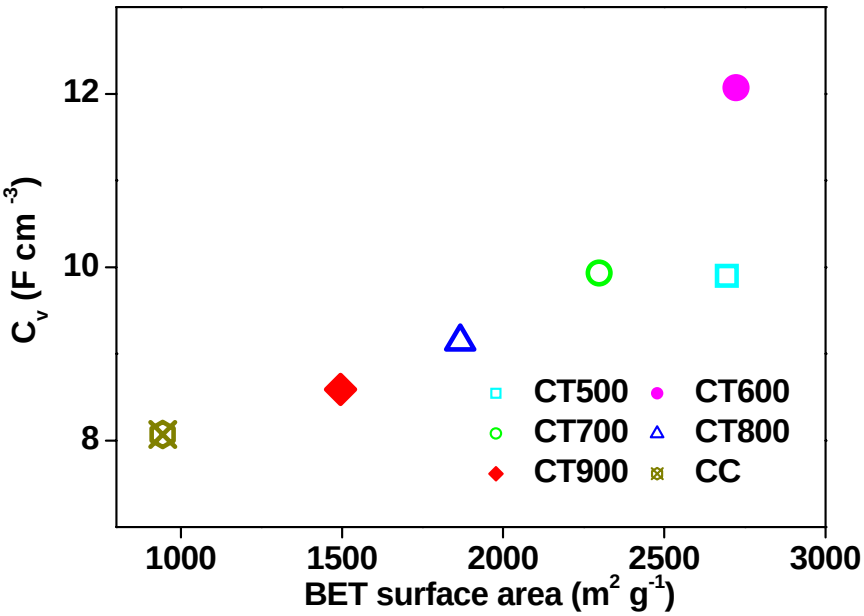


**Figure 3–4** Effect of carbonization temperatures on $C_v$ of ACs

The effect of carbonization temperature on the volumetric capacitance of ACs is also illustrated in **Figure 3–4**. Similar to gravimetric capacitance, as the carbonization temperature increases, the volumetric capacitance of ACs decreases from 600 to 900 $^{o}$C, reaching the maximum value of 12.1 F $cm^{-3}$ at 600 $^{o}$C, larger than CC with the value of

8.1 F $cm^{-3}$. Besides, between the volumetric capacitance and BET surface area also keeps an approximate linear relationship except for the isolation of CT500.

According to the characterization results, 600 $^{o}$C is the most suitable carbonization temperature for obtaining predominant porous carbon with the highest char yield, a higher BET surface area and the highest capacitance than that at other carbonization temperatures. Therefore, the carbonization temperature of 600 $^{o}$C will be used in the next study.

### 3.3.2 Influence of Activation Temperature

The BET surface area and capacitance values corresponding to the ACs obtained at different activation temperatures (500–900 $^{o}$C) but with a fixed carbonization temperature (600 $^{o}$C) are plotted in **Table 3–2**.

**Table 3–2 BET surface area and capacitance of ACs**

| ACs | BET surface area ($m^2$ $g^{-1}$) | Capacitance (F $g^{-1}$) | Capacitance (F $cm^{-3}$) |
|---|---|---|---|
| AT500 | 1935 | 26.1 | 13.8 |
| AT600 | 1910 | 41.4 | 16.6 |
| AT700 | 2613 | 35.8 | 12.0 |
| AT800 | 2723 | 40.8 | 12.1 |
| AT900 | 3089 | 38.1 | 9.0 |
| 600char | 358 | 1.10 | 0.7 |
| CC | 944 | 16.0 | 8.1 |

The BET surface area was found to be increased slowly with the increase of activation temperature. Because the activation reaction with KOH is an endothermic reaction, so the enhancement of temperature is propitious to the process of activation reaction and improves the activation effects. However, the capacitance did not show a propitious relationship with the activation temperature, but keeps a approximate linear relationship with the BET surface area except for AT600. The AC obtained at 900 $^{o}$C shows the highest BET surface area, but a smaller specific capacitance and the smallest volumetric capacitance. The charge-discharge curves are given in **Figure 3–5**.

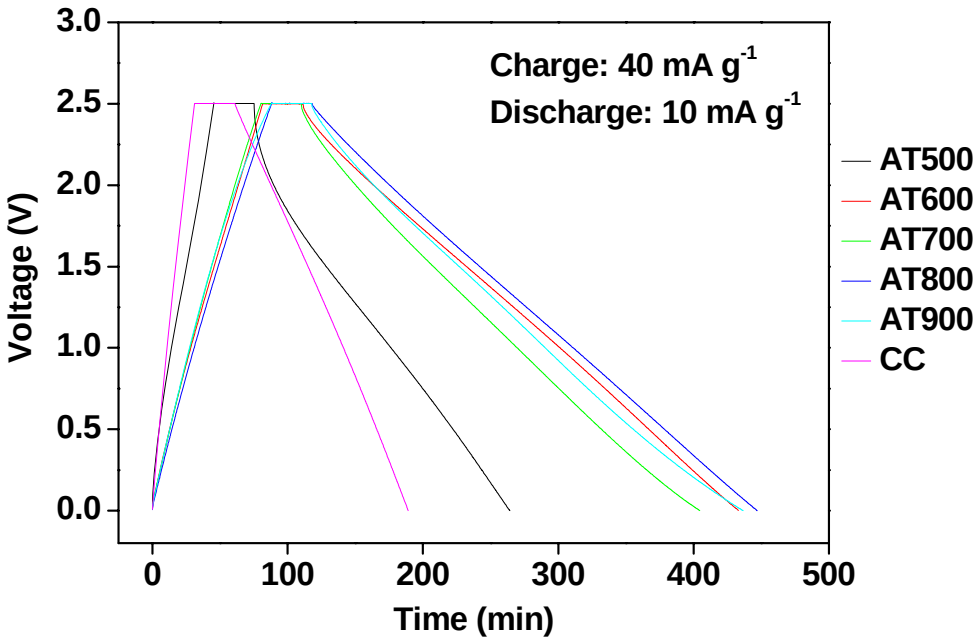


**Figure 3–5 Charge-discharge curves of the ACs-based EDLC**

The effect of activation temperature on capacitance of ACs is illustrated in **Figure 3–6** and **Figure 3–7**. It can be observed that the specific capacitance value as high as 41.4 F $g^{-1}$ and the volumetric capacitance value of 16.6 F $cm^{-3}$ was obtained, which indicates that micropores (pore size less than 2 nm) contribute to the EDLC, and it is also roughly proportional to BET surface area, reaching the maximum value at 600 $^{o}$C.

Besides, the capacitance of 600char is only found to be 0.7 F $cm^{-3}$, which indicates that the pore structure is well improved after the activation process.

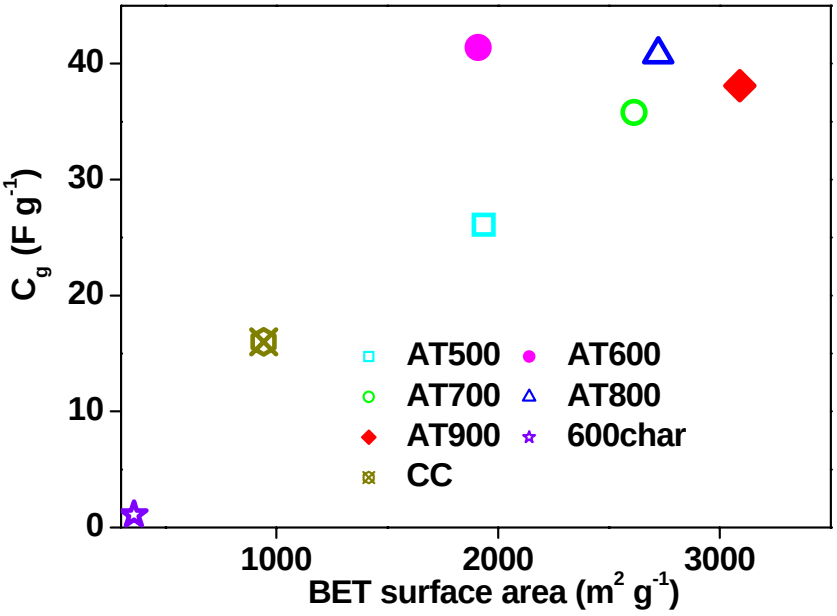


**Figure 3–6 Effect of activation temperatures on $C_g$ of ACs**

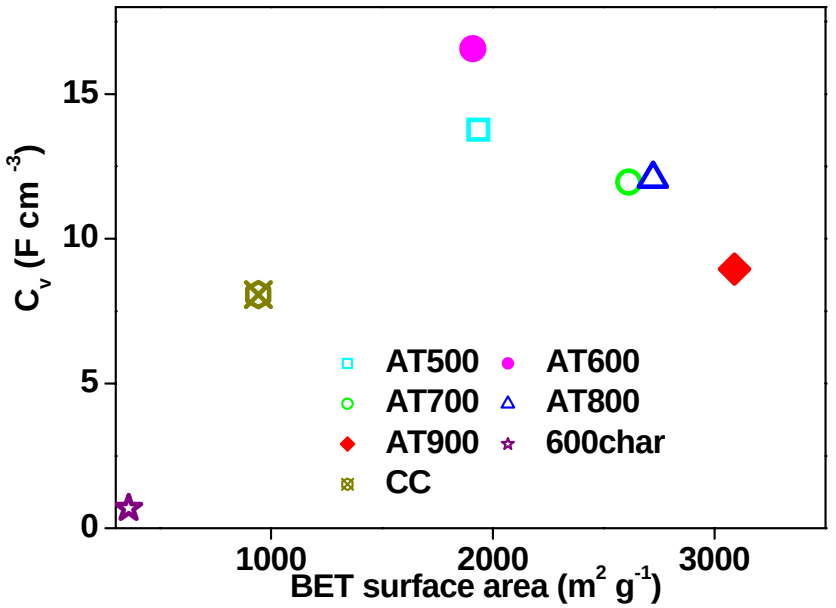


**Figure 3–7 Effect of carbonization temperatures on $C_v$ of ACs**

Besides, there is an inverse proportional relationship between volumetric capacitance and BET surface area. The higher BET surface area, the lower volumetric capacitance, due to the low density of electrode.

### 3.3.3 Influence of Holding Time

**Table 3–3 BET surface area and capacitance of ACs**

| ACs | BET surface area ($m^2\ g^{-1}$) | Capacitance ($F\ g^{-1}$) | Capacitance ($F\ cm^{-3}$) |
|---|---|---|---|
| HT0.5 | 1556 | 37.4 | 15.1 |
| HT1 | 1796 | 38.2 | 15.4 |
| HT1.5 | 1791 | 39.0 | 15.5 |
| HT2 | 1910 | 41.4 | 16.6 |
| HT2.5 | 1936 | 39.5 | 15.3 |
| HT3 | 2140 | 41.0 | 15.7 |
| CC | 944 | 16.0 | 8.1 |

The effect of activation times from 0.5 h to 3 h on BET surface area and capacitance was also investigated, and the result is given in **Table 3–3**. The BET surface area was found to be increased slowly with the increase of holding time, and the specific capacitance and the volumetric capacitance are not very influenced by the holding time, and keeps the values about 37–42 F $g^{-1}$ and 15–17 F $cm^{-3}$, respectively, both larger than the value of CC. The charge-discharge curves are given in **Figure 3–8**.

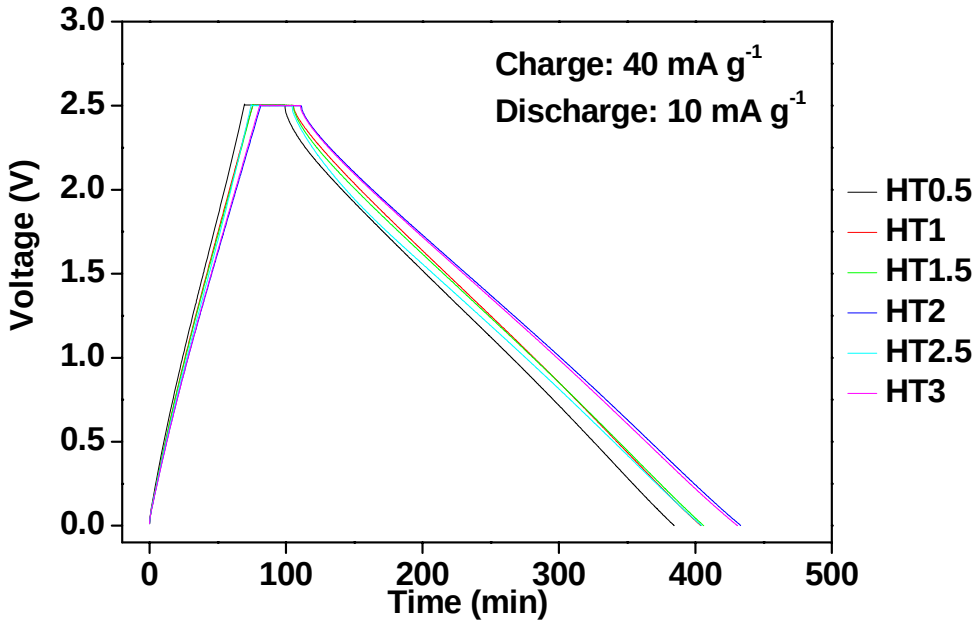


**Figure 3–8 Charge-discharge curves of the ACs-based EDLC**

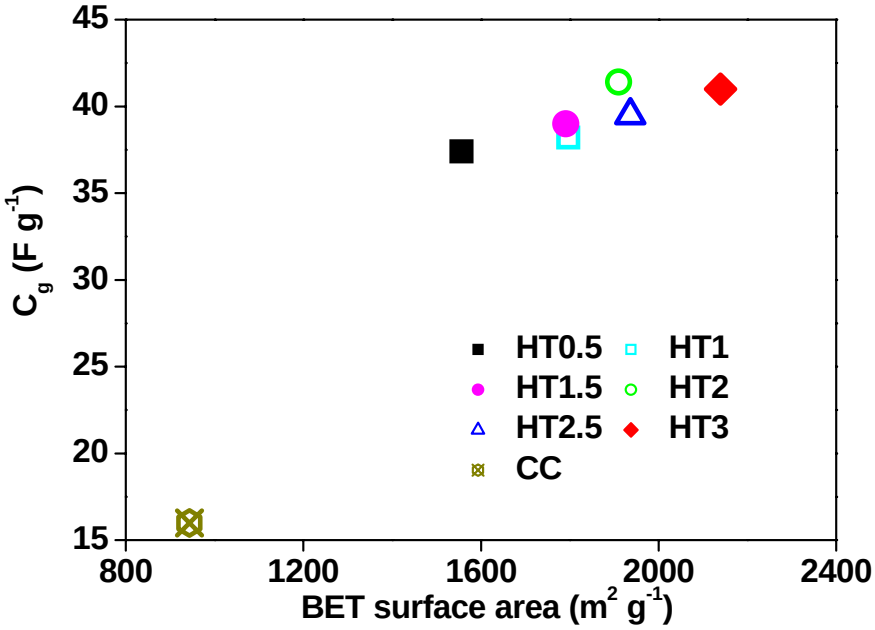


**Figure 3–9 Effect of activation times on $C_g$ of ACs**

**Figure 3–9** and **3–10** show the relationship between the BET surface area and capacitance. It is observed that from 0.5 h to 2 h the specific capacitance and volumetric

capacitance are slightly increased with the increase of holding times, but decreases at 2.5 h and then increases at 3 h lower than that at 2 h. In general, there is a proportional relationship between the specific capacitance and BET surface area, among which HT2 (also named with AT600) shows the highest value, but a little isolation from the linear relationship.

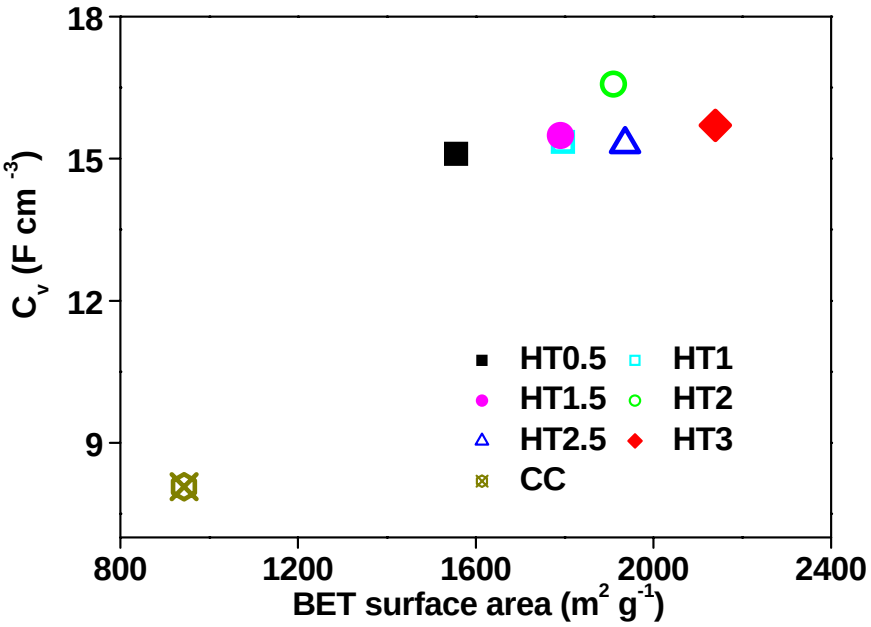


**Figure 3–10 Effect of activation times on $C_v$ of ACs**

## 3.3.4 Influence of Impregnation Ratio

The BET surface area and capacitance values corresponding to the ACs obtained at different impregnation ratios are plotted in **Table 3–4**. IR2 with the highest BET surface area value also shows the largest specific capacitance value of 38.1 F $g^{-1}$, but a low volumetric capacitance value of 9.0 F $cm^{-3}$. However, IR1 with the smallest BET surface area value shows the lowest specific capacitance value of 30.7 F $g^{-1}$, but the largest

volumetric capacitance value of 9.6 F $cm^{-3}$.

**Table 3–4 BET surface area and capacitance of ACs**

| ACs | BET surface area ($m^2$ $g^{-1}$) | Capacitance (F $g^{-1}$) | Capacitance (F $cm^{-3}$) |
|---|---|---|---|
| IR1 | 1936 | 30.7 | 9.6 |
| IR1.5 | 2382 | 34.2 | 9.5 |
| IR2 | 3089 | 38.1 | 9.0 |
| IR2.5 | 2865 | 36.7 | 6.1 |
| IR3 | 2448 | 38.0 | 6.9 |
| CC | 944 | 16.0 | 8.1 |

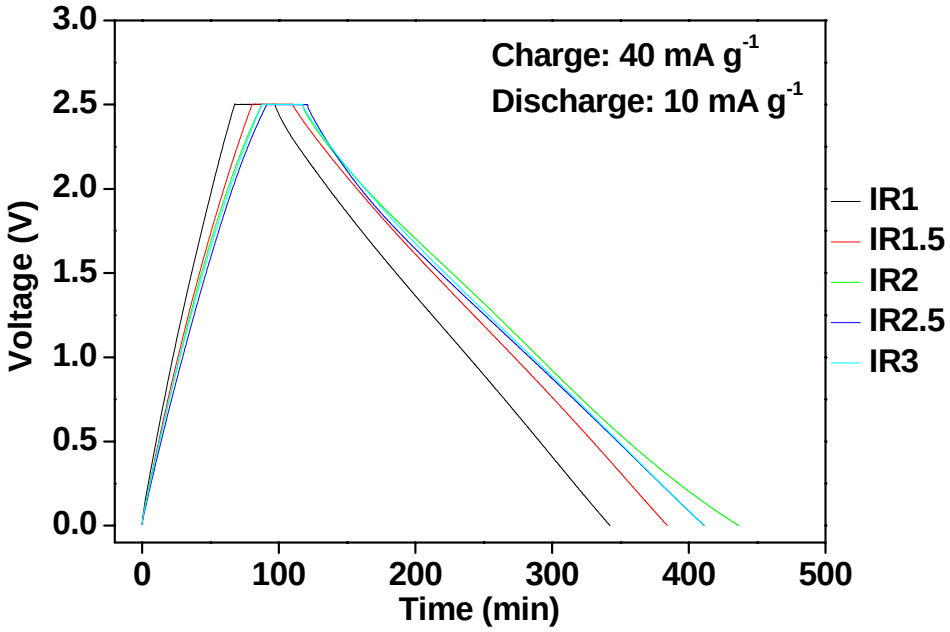


**Figure 3–11 Charge-discharge curves of the ACs-based EDLC**

The charge-discharge curves are given in **Figure 3–11**. **Figures 3–12** and **3–13** show the relationship between the BET surface area and capacitance. It is observed there

is a proportional relationship between the specific capacitance and BET surface area, except for IR3. IR3 has a high capacitance, much higher than the expected value according to the trend.

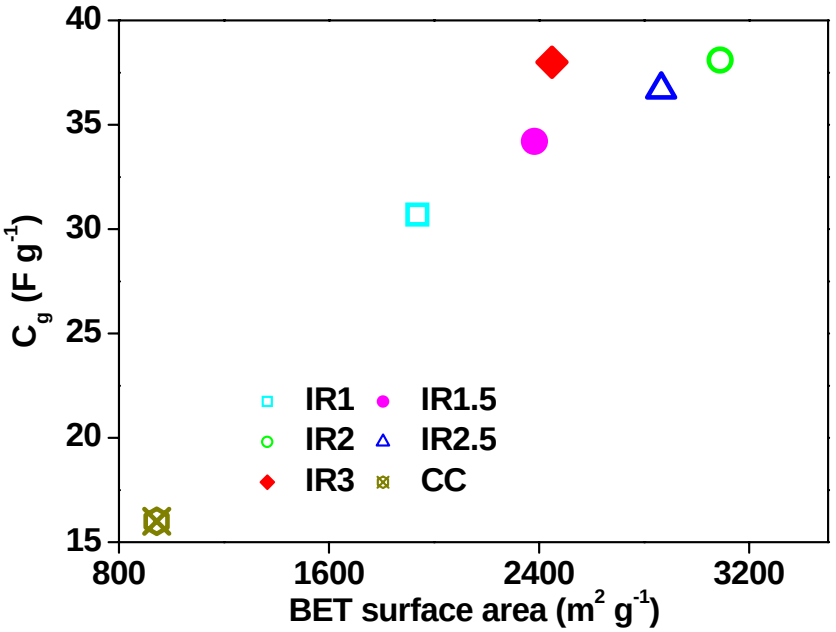


**Figure 3–12 Effect of impregnation ratio on $C_g$ of ACs**

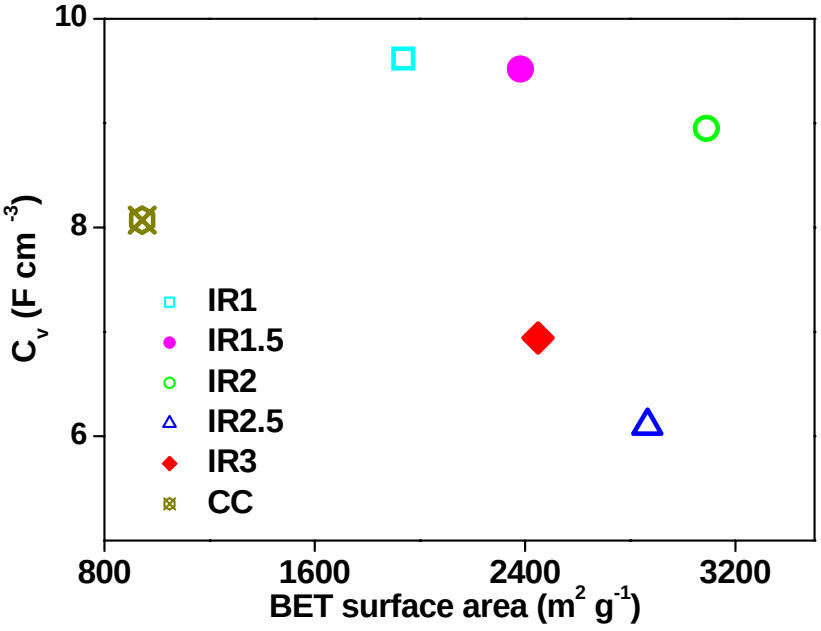


**Figure 3–13 Effect of impregnation ratio on $C_v$ of ACs**

Besides, between the volumetric capacitance there is not a clear relationship, but the volumetric capacitance decreases with the increase of impregnation ratio. And the samples of IR3 and IR2.5 show the lower volumetric capacitance than that of CC.

### 3.3.5 Influence of Activating Agent

Activating agent plays a very important role in the preparation of EDLC from ACs. The effect of different activating agents (KOH, NaOH and $K_2CO_3$) on BET surface area and capacitance was investigated, and the result is given in **Table 3–5**. The three ACs were prepared with the same parameter including carbonization temperature (600 $^oC$), activation temperature (900 $^oC$), holding time (2 h) and impregnation ratio (2). The charge-discharge curves are given in **Figure 3–14**.

**Table 3–5 BET surface area and capacitance of ACs**

| ACs | BET surface area ($m^2\ g^{-1}$) | Capacitance ($F\ g^{-1}$) | Capacitance ($F\ cm^{-3}$) |
|---|---|---|---|
| AT900 | 3089 | 38.1 | 9.0 |
| N900 | 759 | 27.2 | 7.3 |
| K900 | 1136 | 22.2 | 12.2 |
| CC | 944 | 16.0 | 8.1 |

ALL of the ACs exhibit both larger BET surface area and capacitance than CC. AT900 shows the largest BET surface area and highest specific capacitance. Whereas, N900 shows the smallest BET surface area and lowest volumetric capacitance, but a larger specific capacitance than K900. The result indicates that KOH is a very effective

activating agent for preparation AC using for EDLC.

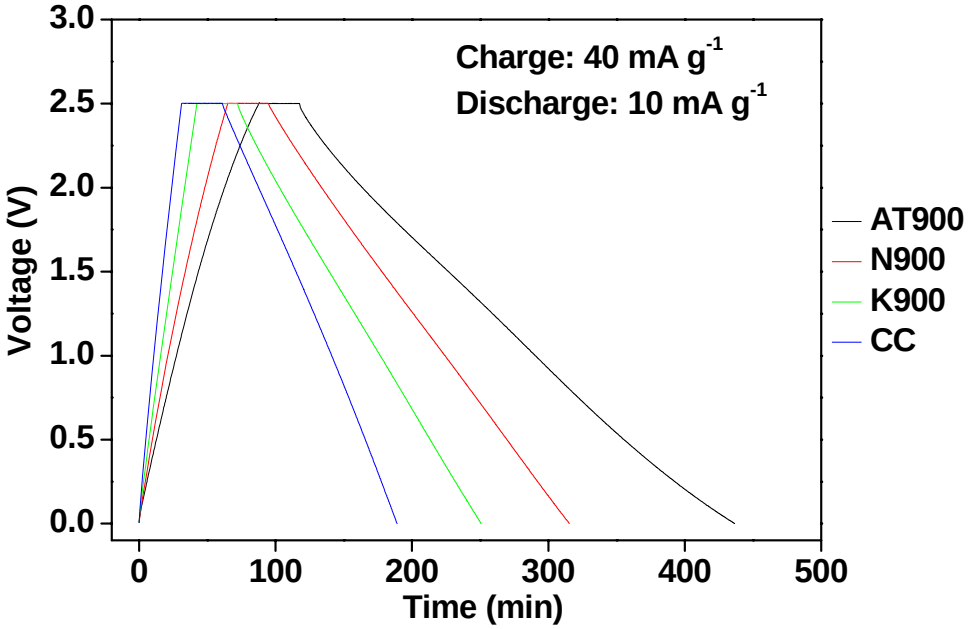


**Figure 3–14 Charge-discharge curves of the ACs-based EDLC**

### 3.3.6 Influence of the Presence of Na and K

In order to investigate the influence of the presence of Na and K, 600 $^{o}$C char was washed by HCl and distilled water until neutral pH to remove the residual alkali metal in black liquor. The BET surface area and capacitance values are plotted in **Table 3–6**, and the charge-discharge curves are given in **Figure 3–15**. According to the result, AT900 shows the higher specific capacitance than ATdaf900, due to its high BET surface area value. It indicates that the presence of Na and K in black liquor did react as activating agent, and the porous structure was well developed which was benefit for the application in EDLC.

**Table 3–6 BET surface area and capacitance of ACs**

| ACs | BET surface area ($m^2\ g^{-1}$) | Capacitance ($F\ g^{-1}$) | Capacitance ($F\ cm^{-3}$) |
|---|---|---|---|
| AT900 | 3089 | 38.1 | 9.0 |
| ATdaf900 | 1245 | 27.2 | 12.8 |

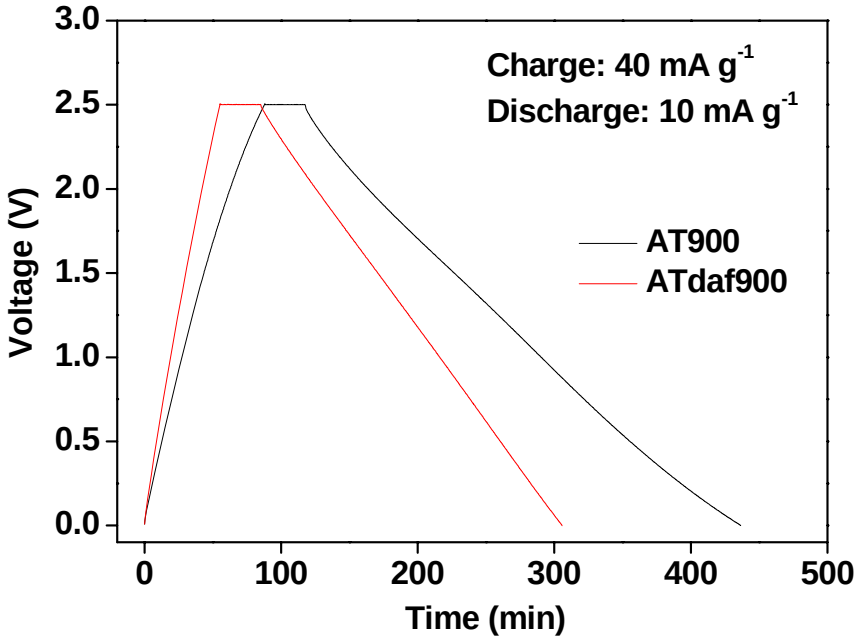


**Figure 3–15 Charge-discharge curves of the ACs-based EDLC**

## 3.3.7 Correlation between EDLC and Pore Sizes

According to the characterization results, a general trend between capacitance and BET surface area exists for all the samples, although it is not a perfect linear relationship. This trend was also observed in previous studies using other carbon materials with lower surface area.[19–21] These results indicate that although the BET surface area is a very important parameter, the EDLC also seems to depend on other characteristics of the

porous carbon materials, probably on the pore size distribution and surface chemistry. As the ACs are obtained from the same precursor and by the same method, they should have similar surface chemistry.

In a previous study,[22] where the EDLC performance of ACs with BET surface areas lower than 2000 $m^2\ g^{-1}$ were measured, it was shown that mesoporosity is beneficial for EDLC. However, for KOH activation, according to the results obtained with samples which show BET surface area larger than 2000 $m^2\ g^{-1}$, it seems that the presence of mesopores in materials with high surface area (> 2000 $m^2\ g^{-1}$) is not very effective for double layer capacitance.

**Figure 3–16** shows the correlations between pore size (≤2 nm) and capacitance, and the correlations between pore size (**>**2 nm) and capacitance is shown in appendix. All ACs with the pore size smaller than 2 nm were displayed in this figure. It was found that there was a peak maximum of capacitance when the pore size was about 1.92 nm, which explained that why AT600 with the pore size of 1.94 nm shows the highest capacitance although its BET surface area is only 1910 $m^2\ g^{-1}$. Capacitance is higher for a sample with wider micropore size distribution than for a sample with higher surface area but too narrow micropore size distribution. Both samples AT600 and AT500 have a similar BET surface area, whereas the capacitance of sample AT600 is much higher than AT500. This different performance of both samples can only be explained considering their pore sizes. As given in **Table 2–2**, AT600 shows a wider micropore size than AT500, even though both samples were prepared by similar conditions. The result shows that the existence of a wider micropore size causes sample AT600 to have a higher capacitance, which fits to

the general trend obtained for the other ACs.

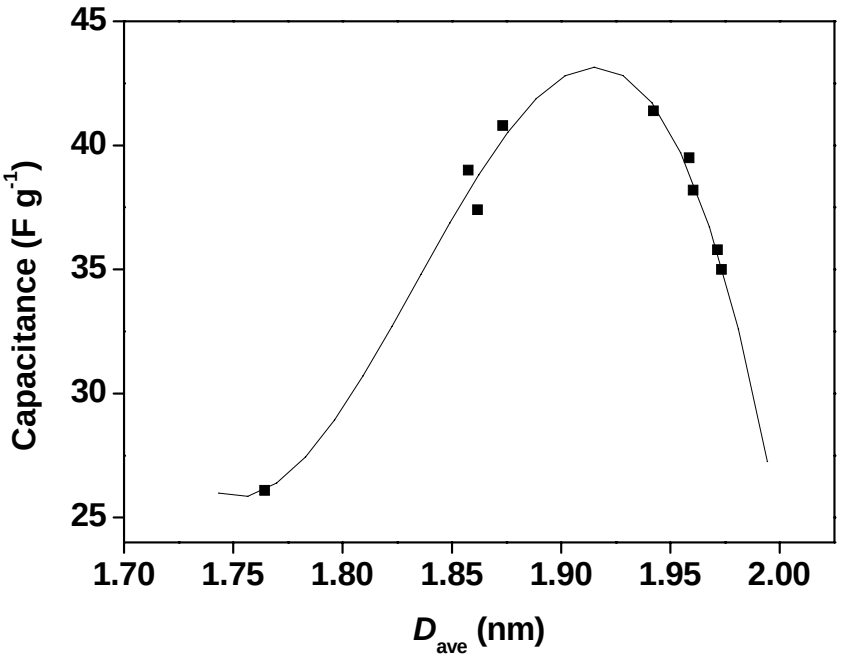


**Figure 3–16 Correlations between pore size (≤2 nm) and capacitance**

The existence of a very small pore size makes the entry of the electrolyte into the pores difficult.[9] Then, the non-accessible pores do not contribute to the total capacitance. Pores of ACs may be incompletely wetted and the small specific capacitance of the AC results from incomplete wetting of pore wall or perturbed double layer. It is believed that pores substantially larger than the size of the electrolyte ion (about 1 nm) and its solvation shell are required for high capacitance. Besides, when pore size is increased, the average distance between pore wall and the center of the ion ($d$) increases and then the capacitance decreases according to

$$C = \epsilon A/d$$

where $A$ is the surface area, d is the separation between carbon and ions, and $\epsilon$ is the local

dielectric constant of the electrolyte. If the pores become even 50% larger than the optimum pore size, there is still room for just one ion per pore, which should be oriented along the longest dimension of the pore. These results show the importance of the accessibility of narrow micropores to electrolytic solution.

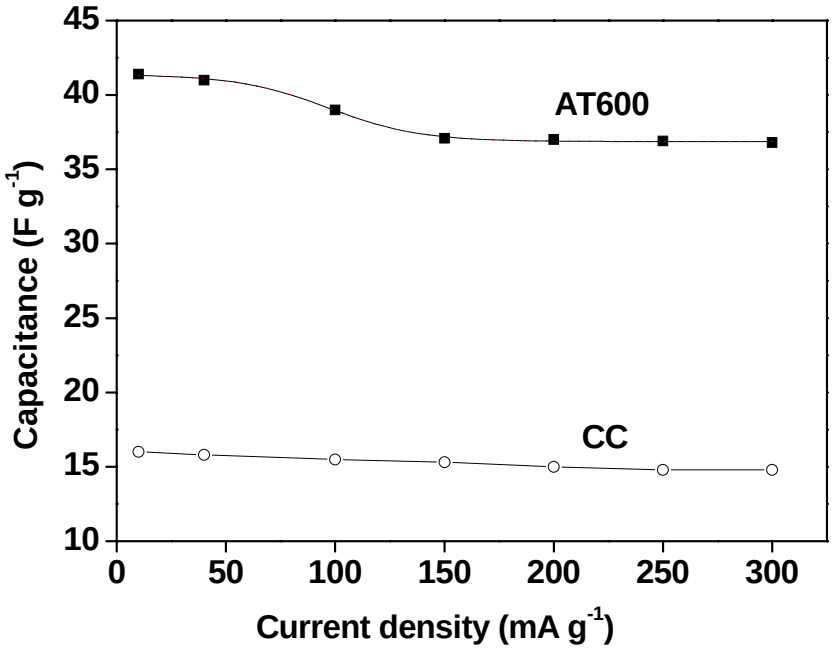


**Figure 3–17 Capacitance against current density**

To characterize the capacitive performance of AC derived from black liquor, **Figure 3–17** exemplifies the capacitance of the sample AT600 and CC in 0.5 M TEABF4/PC as a function of discharge current density. Comparing with CC, AT600 presents a higher capacitance of 41.4 F $g^{-1}$ at a current density of 10 mA $g^{-1}$. In general, the specific capacitance decreases gradually with increasing discharge current density due to large IR drop at a large discharge current density that leads to the small specific capacitance. Although the capacitance decreases slightly with increasing discharge current density, it can still remain as high as 36.8 F $g^{-1}$ at a higher current density of 300 mA $g^{-1}$. The good

performance of AC demonstrates that black liquor will be a promising electrode precursor for EDLC.

## 3.4 Summaries

ACs with high surface area and capacitance derived from black liquor have been prepared by a chemical activation process. The results obtained with ACs of very different surface areas (from 1360 up to 3090 $m^2 g^{-1}$) show that gravimetric capacitance approximately increases with BET surface area, reaching a maximum of 41.4 F $g^{-1}$ for a surface area 1910 $m^2 g^{-1}$. In addition, the results indicate that micropores contribute to the EDLC, and confirm that capacitance not only depends on surface area, but also on pore size distribution. The important microporosity development in the chemically ACs prepared in the present work probably produces a mean micropore size wide (about 1.92 nm) enough to allow the electrolyte access inside the porosity. Besides, the amount of activating agent used in this study was extremely economized comparing with previous researches.[23–24] Accordingly, this study just provides an effective approach to carry out the value-added utilization of black liquor.

## 3.5 References


(1) Qiao, W.M.; Yoon, S.H.; Mochida, I. KOH activation of needle coke to develop activated carbons for high-performance EDLC. *Energy Fuels* **2006**, *20*(4), 1680–1684.

(2) Frackowiak, E.; Béguin, F. Carbon materials for the electrochemical storage of energy in capacitors. *Carbon* **2001**, *39*(6), 937–950.

(3) Qu, Q.T.; Shi, Y.; Tian, S.; Chen, Y.H.; Wu, Y.P.; Holze, R. A new cheap asymmetric aqueous supercapacitor: Activated carbon//$NaMnO_2$. *J. Power Sources* **2009**, *194*(2), 1222–1225.

(4) Shiraishi, S.; Kurihara, H.; Tsubota, H.; Oya, A.; Soneda, Y.; Yamada, Y. Electric double layer capacitance of highly porous carbon derived from lithium metal and polytetrafluoroethylene. *Electrochem. Solid-State Lett.* **2001**, *4*(1), A5–A8.

(5) Wen, Z.B.; Qu, Q.T.; Gao, Q.; Zheng, X.W.; Hu, Z.H.; Wu, Y.P.; Liu, Y.F.; Wang, X.J. An activated carbon with high capacitance from carbonization of a resorcinol–formaldehyde resin. *Electrochem. Commun.* **2009**, *11*(3), 715–718.

(6) Qu, Q.T.; Wang, B.; Yang, L.C.; Shi, Y.; Tian, S.; Wu, Y.P. Study on electrochemical performance of activated carbon in aqueous $Li_2SO_4$, $Na_2SO_4$ and $K_2SO_4$ electrolytes. *Electrochem. Commun.* **2008**, *10*(10), 1652–1655.

(7) Liu, P.; Verbrugge, M.; Soukiazian, S. Influence of temperature and electrolyte on the performance of activated-carbon supercapacitors. *J. Power Sources* **2006**, *156*(2), 712–718.

(8) Rufford, T.E.; Hulicova-Jurcakova, D.; Fiset, E.; Zhu, Z.H.; Lu, G.Q. Double-layer capacitance of waste coffee ground activated carbons in an organic electrolyte. *Electrochem. Commun.* **2009**, *11*(5), 974–977.

(9) Demirbaş, A. Pyrolysis and steam gasification processes of black liquor. *Energy Convers. Manage.* **2002**, *43*(7), 877–884.

(10) Zaied, M.; Bellakhal, N. Electrocoagulation treatment of black liquor from paper industry. *J. Hazard. Mater.* **2009**, *163*(2–3), 995–1000.

(11) Wigmans, T.; Hoogland, A.; Tromp, P.; Moulijn, J.A. The influence of potassium carbonate on surface area development and reactivity during gasification of activated carbon by carbon dioxide. *Carbon* **1983**, *21*(1), 13–22.

(12) Sing, K.S.W.; Everett, D.H.; Haul, R.A.W.; Moscou, L.; Pierotti, R.A.; Rouquerol, J.; Siemieniewska, T. Reporting physisorption data for gas/solid systems, with special reference to the determination of surface area and porosity. *Pure Appl. Chem.* **1985**, *57*(4), 603–619.

(13) Xu, B.; Wu, F.; Su, Y.F.; Cao, G.P.; Chen, S.; Zhou, Z.M.; Yang, Y.S. Competitive effect of KOH activation on the electrochemical performances of carbon nanotubes for EDLC: Balance between porosity and conductivity. *Electrochim. Acta* **2008**, *53*(26), 7730–7735.

(14) Gryglewicz, G.; Machnikowski, J.; Lorenc-Grabowska, J.E.; Lota, G.; Frackowiak, E. Effect of pore size distribution of coal-based activated carbons on double layer capacitance. *Electrochim. Acta* **2005**, *50*(5), 1197–1206.

(15) Lozano-Castelló, D.; Cazorla-Amorós, D.; Linares-Solano, A.; Shiraishi, S.;

Kurihara, H.; Oya, A. Influence of pore structure and surface chemistry on electric double layer capacitance in non-aqueous electrolyte. *Carbon* **2003**, *41*(9), 1765–1775.

(16) Barbier, O.; Hahn, M.; Herzog, A.; Kötz, R. Capacitance limits of high surface area activated carbons for double layer capacitors. *Carbon* **2005**, *43*(6), 1303–1310.

(17) Endo, M.; Maeda, T.; Takeda, T.; Kim, Y.J.; Koshiba, K.; Hara, H.; Dresselhaus, M.S. Capacitance and pore-size distribution in aqueous and nonaqueous electrolytes using various activated carbon electrodes. *J. Electrochem. Soc.* **2001**, *148*(8), A910–A914.

(18) Salitra, G.; Soffer, A.; Eliad, L.; Cohen, Y.; Aurbach, D. Carbon electrodes for double-layer capacitors I. Relations between ion and pore dimensions. *J. Electrochem. Soc.* **2000**, *147*(7), 2486–2493.

(19) Tanahashi, I.; Yoshida, A.; Nishino, A. Properties of the electric double layer capacitors composed of activated carbon fiber cloth electrodes and a organic electrolyte. *Denki Kagaku* **1988**, *56*(10), 892–897.

(20) Morimoto, T.; Hiratsuka, K.; Sanada, Y.; Kurihara, K. Electric double-layer capacitor using organic electrolyte. *J. Power Sources* **1996**, *60*(2), 239–247.

(21) Lin, C.; Ritter, J.A.; Popov, B.N. Correlation of double-layer capacitance with the pore structure of sol-gel derived carbon xerogels. *J. Electrochem. Soc.* **1999**, *146*(10), 3639–3643.

(22) Shiraishi, S.; Kurihara, H.; Shi, L.; Nakayama, T.; Oya, A. Electric double-layer capacitance of meso/macroporous activated carbon fibers prepared by the blending

method. *J. Electrochem. Soc.* **2002**, *149*(7), A855–A861.

(23) Mitani, S.; Lee, S.I.; Yoon, S.H.; Korai, Y.; Mochida, I. Activation of raw pitch coke with alkali hydroxide to prepare high performance carbon for electric double layer capacitor. *J. Power Sources* **2004**, *133*(2), 298–301.

(24) Lillo-Ródenas, M.A.; Cazorla-Amorós, D.; Linares-Solano, A. Understanding chemical reactions between carbons and NaOH and KOH: An insight into the chemical activation mechanism. *Carbon* **2003**, *41*(2), 267–275.

# Chapter 4 Conclusions

High surface area ACs were prepared from chemical activation of black liquor with KOH, NaOH and $K_2CO_3$. Black liquor was found to be a good raw material for developing ACs with favorable pore characteristics. The results obtained with ACs of very different surface areas (from 1360 up to 3090 $m^2 g^{-1}$) show that the porosity of ACs is highly dependent on the preparation conditions, such as carbonization temperature, activation temperature, holding time and chemical impregnation ratio. Under the experimental conditions studied, the best conditions for preparing ACs with high surface area and pore volume are a carbonization temperature of 600 $^oC$, an activation temperature of 900 $^oC$, and an impregnation ratio of 2 (KOH to char). With these experimental conditions, an AC with a BET surface area of 3089 $m^2 g^{-1}$ and a total pore volume of 1.76 $cm^3 g^{-1}$ was obtained. Furthermore, the optimal impregnation ratio of 2 is much lower than those recommended in the literature. Too high of an impregnation ratio results in the burn-off of carbon structures and widening of the micropores. The amount of activating agent used in this study was extremely economized compared with previous studies. Accordingly, black liquor has been demonstrated to be an excellent and low-cost candidate for manufacturing ACs with favorable pore characteristics.

Besides, the results show that gravimetric capacitance approximately increases with surface area, reaching a maximum of 41.4 F $g^{-1}$ for a surface area 1910 $m^2 g^{-1}$. In addition, the results indicate that micropores contribute to the EDLC, and confirm that

capacitance not only depends on surface area, but also on pore size distribution. The important microporosity development in the chemically ACs prepared in the present work probably produces a mean micropore size wide (about 1.92 nm) enough to allow the electrolyte access inside the porosity. The volumetric capacitance don't show a clear relationship with surface area, but also larger than the value of CC. Accordingly, this study just provides an effective approach to carry out the value-added utilization of black liquor.

# Acknowledgements

First, I would like to express my sincere gratitude to my advisor, Professor Takayuki Takarada, for his advice, guidance, encouragement and assistance throughout this study. The challenging ideas and thought-provoking discussion contributed greatly throughout the course of this study. I also own very special thanks to my co-advisor Professor Xian-Yong Wei, from China University of Mining & Technology, for his close advice and assistance in this study. Without him I would not have been here in the first place. I am grateful to the committee members, Professors Shinji Katsura, Jun-ichi Ozaki, Masaru Hakoda, and Reiji Noda for their advice, support and review of my thesis.

I would also express my appreciation to other faculty members, staffs and graduated students in Prof. Takarada's laboratory for their help with my research work. Particularly, I would like to thank Drs. Koyoko Morishita and Kazuyoshi Sato for their encouragements and assistance; the technical staff, Ms. Yukiko Ogawa, for her kindly help on sample analyses, and to Ms. Miyoko Kakuage and Ms. Mayumi Tanaka, for their help related to this work. In addition, I would like to thank Drs. Liu-Yun Li, Xian-Bin Xiao and Shou-Yu Zhang for their assistance and friendship.

I would also like to acknowledge China Scholarship Council (Project No. [2007]3020) for financial support.

Most of all, I am greatly indebted to my husband Jin-Pei Cao, who is also a Ph.D

student in Gunma University, for his encouragement and support in this work. Many thanks to my baby son (he was born in beginning of this year) for all his smiles and love. Also, I would like to thank my beloved parents and parents-in-low for their consistent support, encouragement and help for take care of my son. I owe my every achievement to my family.

Xiao-Yan Zhao

5/12/2010

# List of Publications


[1] **Xiao-Yan Zhao**, Jing-Pei Cao*, Kayoko Morishita, Jun-ichi Ozaki, Takayuki Takarada.. Electric Double-Layer Capacitors from Activated Carbon Derived from Black Liquor. *Energy Fuels*, **2010**, 24(3), 1889–1893.

[2] **Xiao-Yan Zhao**, Jing-Pei Cao*, Kazuyoshi Sato, Yukiko Ogawa, Takayuki Takarada. High Surface Area Activated Carbon Prepared from Black Liquor in the Presence of High Alkali Metal Content. *Journal of Chemical Engineering of Japan*, **2010**, 43(12), 1029–1034.

[3] Jing-Pei Cao*, **Xiao-Yan Zhao**, Kayoko Morishita, Liu-Yun Li, Xian-Bin Xiao, Ryoji Obara, Xian-Yong Wei, Takayuki Takarada. Triacetonamine formation in a bio-oil from fast pyrolysis of sewage sludge using acetone as the absorption solvent. *Bioresource Technology*, **2010**, 101(11): 4242–4245.

[4] Jing-Pei Cao*, **Xiao-Yan Zhao**, Kayoko Morishita, Xian-Yong Wei, Takayuki Takarada. Fractionation and identification of organic nitrogen species from bio-oil produced by fast pyrolysis of sewage sludge. *Bioresource Technology*, **2010**, 101(19): 7648–7652.

[5] Jing-Pei Cao*, Xian-Bin Xiao, Shou-Yu Zhang, **Xiao-Yan Zhao**, Kazuyoshi Sato, Yukiko Ogawa, Xian-Yong Wei, Takayuki Takarada. Preparation and characterization

of bio-oils from internally circulating fluidized-bed pyrolysis of municipal, livestock and wood waste. *Bioresource Technology*, **2011**, 102, (2), 2015-2021.

[6] Jing-Pei Cao*, Liu-Yun Li, Kayoko Morishita, Xian-Bin Xiao, **Xiao-Yan Zhao**, Xian-Yong Wei, Takayuki Takarada. Nitrogen transformations during fast pyrolysis of sewage sludge. *Fuel*, **2010**, doi: 10.1016/j.fuel.2010.08.015.

# List of Presentations

[1] **Xiao-Yan Zhao**, Kayoko Morishita, Takayuki Takarada. Electric double layer capacitors from activated carbon derived from black liquor. *The 10$^{th}$ Japan-China symposium on coal and $C_1$ chemistry*. July 26-29, 2009, Tsukuba, Ibaraki, Japan; E06.

[2] **Xiao-Yan Zhao**, Kayoko Morishita, Takayuki Takarada. Preparation of EDLC using black liquor. *The 41$^{st}$ Autumn Meeting of the Society of Chemical Engineers*, *Japan*. Sep 16–18, 2009, Higashi-Hiroshima, Japan; AA107.

# Appendix

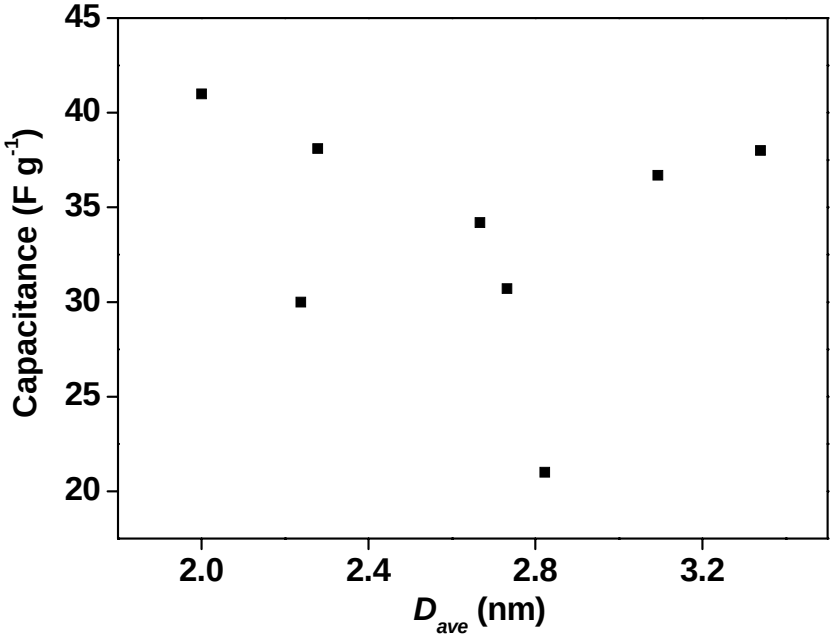


**Figure 3-18 Correlations between pore size (>2 nm) and capacitance**

# List of Abbreviations

| | |
|---|---|
| KOH | potassium hydroxide |
| NaOH | sodium hydroxide |
| $K_2CO_3$ | potassium carbonate |
| BLGMF | black liquor gasification with motor fuels production |
| DME | dimethyl ether |
| AC | activated carbon |
| EDLC | electric double layer capacitor |
| LIB | lithium ion battery |
| MPCF | mesophase pitch-based carbon fiber |
| IPCF | isotropic pitch-based carbon fiber |
| HCl | hydrochloric acid |